Static Load Cycle Testing of a Very Low-Aspect-Ratio Six-Inch Wall TRG-Type Structure TRG-6-6 (0.27, 0.50)

Prepared by
C. R. Farrar, J. G. Bennett, W. E. Baker, W. E. Dunwoody

Los Alamos National Laboratory

Static Load Cycle Testing of a Very Low-Aspect-Ratio Six-Inch Wall TRG-Type Structure TRG–6–6 (0.27, 0.50)

Prepared by
C. R. Farrar, J. G. Bennett, W. E. Baker*, W. E. Dunwoody

Los Alamos National Laboratory
Los Alamos, NM 87545

*Consultant, University of New Mexico, Albuquerque, NM 87131

PREVIOUS REPORTS IN THE SERIES

E. G. Endebrock and R. C. Dove, "Seismic Response of Nonlinear Systems," Los Alamos National Laboratory report LA-8981-MS, NUREG/CR-2310 (September 1981).

E. G. Endebrock, R. C. Dove, and C. A. Anderson, "Margins to Failure - Category I Structures Program: Background and Experimental Plan," Los Alamos National Laboratory report LA-9030-MS, NUREG/CR-2347 (December 1981).

E. G. Endebrock, R. C. Dove, and W. E. Dunwoody, "Analysis and Tests on Small-Scale Shear Walls--FY 82 Final Report," Los Alamos National Laboratory report LA-10443-MS, NUREG/CR-4274 (September 1985).

R. C. Dove and J. G. Bennett, "Scale Modeling of Reinforced Concrete Category I Structures Subjected to Seismic Loading," Los Alamos National Laboratory report LA-10624-MS, NUREG/CR-4474 (January 1986).

R. C. Dove, J. G. Bennett, C. Farrar, and C. A. Anderson, "Seismic Category I Structures Program Final Report, FY 1983-84," Los Alamos National Laboratory report LA-11013-MS, NUREG/CR-4924 (September 1987).

J. G. Bennett, R. C. Dove, W. E. Dunwoody, E. G. Endebrock, C. R. Farrar, and P. Goldman, "Simulated Seismic Tests on 1/42- and 1/14-Scale Category I, Auxiliary Buildings," Los Alamos National Laboratory report LA-11093-MS, NUREG/CR-4987 (October 1987).

J. G. Bennett, R. C. Dove, W. E. Dunwoody, C. R. Farrar, and P. Goldman, "The Seismic Category I Structures Program: Results for FY 1985," Los Alamos National Laboratory report LA-11117-MS, NUREG/CR-4998 (December 1987).

C. R. Farrar and J. G. Bennett, "Experimental Assessment of Damping in Low Aspect Ratio, Reinforced Concrete Shear Wall Structures," Los Alamos National Laboratory report LA-11325-MS, NUREG/CR-5154 (August 1988).

J. G. Bennett, R. C. Dove, W. E. Dunwoody, C. R. Farrar, and P. Goldman, "The Seismic Category I Structures Program: Results for FY 1986," Los Alamos National Laboratory report LA-11377-MS, NUREG/CR-5182 (September 1988).

C. R. Farrar and C. M. Alvord, "Use of Linear Reduced-Stiffness Analytical Models to Predict Seismic Response of Damaged Concrete Structures," Los Alamos National Laboratory report LA-11444-MS, NUREG/CR-52_7 (May 1989).

C. R. Farrar, J. G. Bennett, W. E. Dunwoody, and W. E. Baker, "Static Load Cycle Testing of a Low-Aspect-Ratio Six-Inch Wall, TRG-type Structure TRG-4-6 (1.0, 0.25)," Los Alamos National Laboratory report LA-11422-MS, NUREG/CR-5222 (June 1989).

ABSTRACT

This test report is the third for a series of tests carried out by the Los Alamos National Laboratory under the sponsorship of the United States Nuclear Regulatory Commission's Division of Engineering. This research program has a Technical Review Group that recommended test geometries and sizes for the tests.

The quasi-static load cycle testing of a totally shear-dominated structure (bending deformation negligible) made of 6-inch-thick reinforced concrete walls is reported herein. The background of the program and the results that led to this series of experiments is first reviewed for continuity. Next, the geometry of the test structure, the design parameters, and the construction of the structure, including the material property tests, are reported. Both modal analysis and modal testing were done to verify the undamaged dynamic properties of the structure. Finally, the results of the quasi-static cyclic testing are reported in detail.

Results are compared with other investigations and with the American Concrete Institute (ACI) 349-85 code predictions.

TABLE OF CONTENTS

APPENDICES

LIST OF FIGURES

LIST OF TABLES

STATIC LOAD CYCLE TESTING OF A ~~.~ (LOW-ASPECT-RATIO
SIX-INCH WALL TRG-TYPE STRUCTURE TRG-6-6
(0.27, 0.50)

by

Charles R. Farrar, Joel G. Bennett,
William E. Baker, and Wade E. Dunwoody

I. INTRODUCTION

Previous work that has been carried out at Los Alamos National Laboratory (LANL) as part of the Seismic Category I Structures Program for the United States Nuclear Regulatory Commission (USNRC) Office of Nuclear Regulatory Research has consistently measured reductions in stiffness of four or more in scale models of low aspect ratio shear wall structures subjected to working loads. In this context, working loads refer to load levels equivalent to those experienced by a structure during an operating basis earthquake that would produce stresses on the order of 50-psi average base shear. The models tested thus far have been made of both microconcrete and conventional concrete and have been tested statically and dynamically.

Upon review of these results at the Technical Review Group (TRG) meeting of April 4, 1986, it was decided to conclude the experimental investigation of the reduced stiffness issue[*] by performing a series of quasi-static load cycle tests on structures with a cross-sectional geometry similar to the TRG-3-4 (1.0, 0.56) structure.

The nomenclature used here is as follows:

TRG-No.-Wt (AR,%R),

where,

TRG = the designation for the series of structures designed and tested using
        guidance from the program's Technical Review Group, a group of nationally
        recognized nuclear structural experts,
No. = the sequence number in the series,
Wt = the shear wall thickness,
AR = the height-to-length aspect ratio of the shear wall, and
%R = total percentage by area of steel reinforcing in both directions.

---

[*] See the Background Section for a brief explanation of why the program has
    deviated from initial objectives to investigate the reduced stiffness
    issue.

Thus, this letter report concerns TRG-6-6 (0.27, 0.50). The test structures were to be constructed with different aspect ratios and reinforcement percentages so that variations in these parameters that exist in actual Category I structures could be taken into account in the experiments and the sensitivity to these variables could be identified.

One of the primary purposes of these tests was to determine if, at equivalent stress levels, a similar reduction in stiffness occurs during static testing as has been observed during the dynamic testing.* In addition, the structures were to be instrumented so that the contribution to bending stiffness of the flexural boundary elements (shear walls in orthogonal planes) could be assessed. The structures were also instrumented so that the shear and bending contributions to the total stiffness could be measured separately. The separation of shear and bending components of stiffness was intended to provide additional information concerning the mechanism for the reduction in stiffness.

II. BACKGROUND

The purpose of this report is to provide the USNRC, the TRG, as well as the civil structure community with a summary of the principal results and conclusions from an experiment on a very low aspect ratio, 6-in. wall, TRG-type structure. This structure was quasi-statically tested as part of the Seismic Category I Structures Program. However, for the reader who may be unaware of this program or who wishes to review the program objectives and history, a summary will be provided.

The Seismic Category I Structures Program is being carried out at Los Alamos National Laboratory under sponsorship of the USNRC, Office of Nuclear Regulatory Research, and has the objective of investigating the structural dynamic response of Seismic Category I reinforced concrete structures (exclusive of containment) that are subjected to seismic loads beyond the design basis.

A number of meetings and interactions with the NRC staff have led to a set of specific program objectives, which are as follows:

1. to address the seismic response of reinforced concrete Category I structures, other than containment structures;

2. to develop experimental data for determining the sensitivity of structural behavior, in the elastic and inelastic response range, to variations in configuration, design practices, and earthquake loading;

3. to develop experimental data to enable validation of computer programs used to predict the behavior of Category I structures during earthquake motions that cause elastic and inelastic response;

_____

*Previous comparisons between static and dynamic tests of isolated shear walls, 1/30-scale, single-story, diesel generator buildings, TRG-1-1 (1.0, 0.5) and TRG-3-4 (1.0, 0.56) have, in fact, shown the opposite. That is, the reduction in stiffness was much more pronounced in dynamic tests than it was in static tests at similar average base shear stress levels. However, these structures with the exception of TRG-3 were all small-scale microconcrete models.

2

4.   to identify floor response spectra changes that occur during earthquake motions that cause elastic and inelastic structural response;

5.   to develop a method for representing damping in the inelastic range and to demonstrate the way in which this damping changes when structural response goes from the elastic to the inelastic ranges; and

6.   to assess how shifts in structural frequency affect plant risk.

A principal characteristic of the typical structure under investigation is that shear rather than flexure is dominant; that is, the ratio of displacement values calculated from terms identified with shear deformation to the values contributed from bending deformation is one or greater. Thus, these buildings are called "shear wall" structures.

The Seismic Category I Structures Program began in FY 1980 with an investigation that identified the typical shear wall structure, its characteristics (stiffnesses, frequencies, etc.), and areas in which nuclear design firms [Bechtel Corporation, Sargent & Lundy, and Tennessee Valley Authority (TVA)] felt additional experimental data were needed. A combined experimental/analytical plan for investigation of the dynamic behavior of these structures was prepared (Ref. 1). During the first phase, the program concentrated on investigating isolated shear wall behavior using small models (1/30-scale) that could be economically constructed and tested both statically and dynamically. Also, during this phase of the program, a TRG, consisting of nationally recognized seismic and concrete experts on nuclear civil structures, was established both to review the progress and make recommendations regarding the technical directions of the program. The recommendations of this group have been evaluated in light of the needs of the USNRC and, when possible, have been carefully integrated into the program.

Following the isolated shear wall phase, the program began testing and evaluating three-dimensional box-like model structures. It was recognized from the outset that scale-model testing of concrete structures is a controversial issue in the U.S. civil engineering community. Thus, with the testing of small-scale test structures, a task of demonstrating scalability of the results to prototype structures was initiated. The details and results of these investigations are reported in Refs. 2-6.

To give a brief synopsis of the situation at the end of FY 1984, the program had tested (in addition to the isolated shear walls), either statically or seismically, 23 different models representing 2 types of structures, a diesel generator building, and an auxiliary buildirg. Two different scales [(1/30, 1/10) and (1/42, 1/14)] of these buildings were used (1-in. and 3-in. walls). In addition, stories varied from one to three. Although a number of results on items, such as aging (cure time), effect of increasing seismic magnitude, etc., have been reported, two important and consistent conclusions came out of the data from these tests. First, the scalability of the results was illustrated both in the elastic and inelastic range. Second, the so-called "working load" secant stiffness of the models was lower than was the computed uncracked cross-sectional values by a factor of about 4.

During their review, the TRG pointed out the following:

1. Design of prototype nuclear plant structures is normally based upon an uncracked cross-section strength-of-materials approach that may or may not use a "stiffness reduction factor" for the concrete. But, if one is used, it is never as large as 4.

2. Although the structures themselves appear to have adequate reserve margin (even if the stiffness is only 25% of the theoretical), any piping and attached equipment will have been designed using inappropriate floor response spectra.

3. Given that a nuclear structure designed to have a natural response of about 15 Hz really has a natural frequency of 7.5 Hz (corresponding to a reduction in stiffness of 4) and allowing further that the natural frequency will decrease because of degrading stiffness, the natural response of the structure will shift well down into the frequency range for which an earthquake's energy content is the largest. This will result in increased amplification in the floor response spectra at lower frequencies, and this fact potentially has significant impact on the equipment and on the piping design response spectra and their margins of safety.

Note that all three points are related to the difference between the measured and calculated stiffnesses of these structures.

Having made these observations, several questions arose. Did our previous experimental data taken on microconcrete models represent behavior that would be observed in prototype structures? What is the appropriate value of the stiffness that should be used in design and for component response spectra computations in these structures? Should this value be a function of load level? Have the equipment and piping in existing buildings been designed to inappropriate response spectra?

Thus, the primary program emphasis at that time was to ensure credibility of previous experimental work by beginning to resolve the "stiffness difference" issue. The TRG for this program believed that this important issue must be addressed before the program objectives could be accomplished.

To address these stiffness-related concerns, it was agreed that a series of credibility experiments was to be carried out using both large- and small-scale structures. For the large-scale structure, the TRG set limitations on design parameters. The recommended "ideal" structure characteristics, in order of decreasing priority, were as follows:

1. Maximum predicted bending and shear mode natural frequency ≤ 30 Hz,
2. Minimum wall thickness - 4 in.,
3. Height-to-depth ratio of shear wall ≤ 1,
4. Use actual No. 3 rebar for reinforcing,
5. Use realistic material for aggregate,
6. Use 0.1%-1% steel (0.3% each face, each direction, i.e., 0.6% total each direction), and
7. Use water-blasted construction joints to ensure good aggregate interlock.

A prototype "TRG" structure, of the same geometry shown in Fig. 1, but having 4-in. walls and an aspect ratio of 1, and designed to comply with these specifications, was constructed using actual batch plant concrete and No. 3 rebar. In addition, a 1/4-scale model of the TRG structure was constructed with microconcrete and wire-mesh rebar and was tested prior to the prototype. Both structures were tested statically (80 psi principal tensile stress for the 1/4-scale, 40 psi for the prototype) and then seismically to failure, or in the case of the prototype, to machine limits.
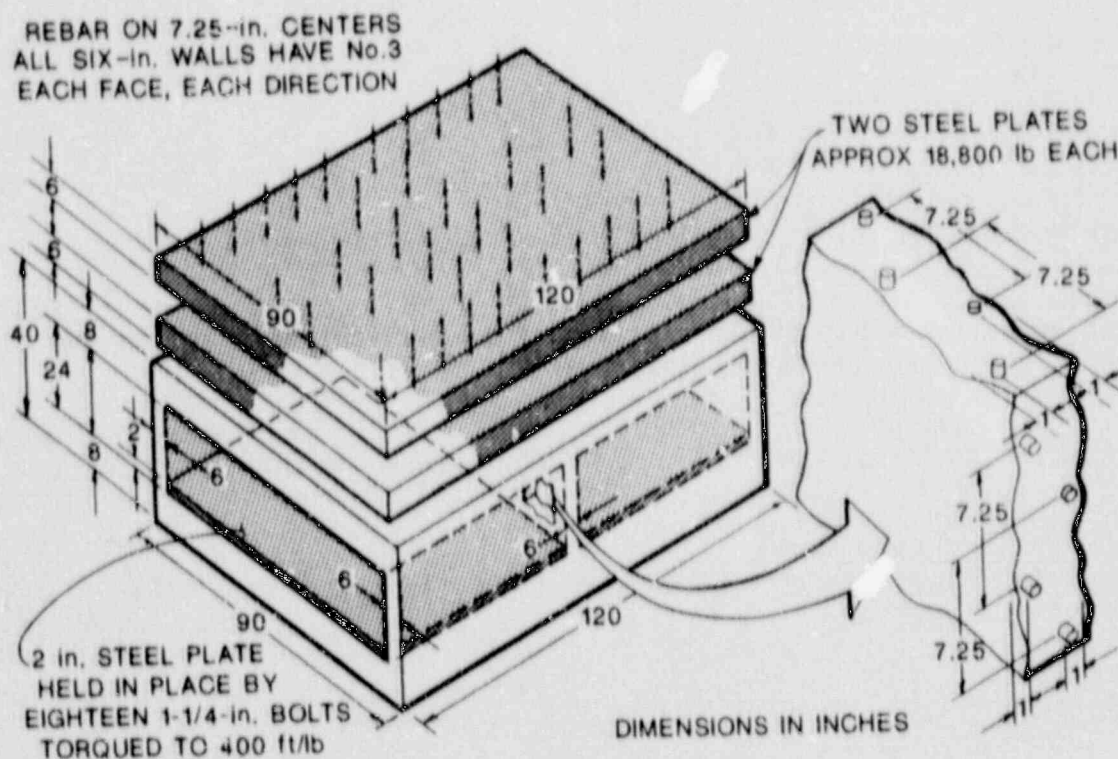
Fig. 1.   TRG-6 test structure.

These tests were intended to show that the previously observed reductions in stiffness were not related to the use of microconcrete and that the static and dynamic test results of the microconcrete models could be scaled to conventional concrete structures.

During the static tests, the 1/4-scale model, TRG-1-1 (1.0, 0.6), showed results similar to those of the prototype, TRG-3-4 (1.0, 0.56), for stiffness and suggested that, for low-level static response, the microconcrete model did an adequate job of predicting the response of the conventional concrete prototype. A low-force-level experimental modal analysis performed prior to the seismic excitation showed stiffness and scalability results similar to those of the static test.

When the structures were tested dynamically on a shake table, both models showed reductions in stiffness consistent with previous test data, thus suggesting that the reduced stiffness could not be attributed to microconcrete. An extensive

5

analytical investigation was made to determine if the measured reductions in stiffness found while testing TRG-3 could be attributed to base connection effects. From this investigation, it was concluded that the base connections were not responsible for the measured stiffness reductions. The prototype TRG structure with its added mass was large enough to make reproduction of the input signal impossible. This input signal was meant to be a scaled version of the one used on the 1/4-scale model, but, because it could not be accurately reproduced (frequency content of the signal was distorted), conclusions concerning the scalability of seismic response between the conventional concrete prototype and the microconcrete model could not be made. The results of these tests and the analytical investigation of base connection effects appear in detail in Ref. 7.

One variable in the TRG-3 test that could not be assessed was the effects of shipping and handling. The structure was constructed in Los Alamos and shipped by truck to Champaign, Illinois, for testing. The TRG-4, -5, and -6 structures were constructed at Los Alamos and tested with a minimum of handling.

Stiffness values measured on TRG-4-6 (1.0, 0.25) and TRG-5-4 (1.0, 0.1) were repeatable and were almost identical to the theoretical values until the structure first cracked. The stiffness components attributable to shear and bending were separated and were found to agree almost exactly with theory. After cracking, the stiffness degraded during load cycling. The amount of degradation was found to be a function of previous load history and the amount of reinforcement.

III. REVIEW OF PREVIOUS STATIC TEST RESULTS OBTAINED IN THE SEISMIC CATEGORY I STRUCTURES PROGRAM

Previously in this program, measured stiffness values from static and dynamic tests have been compared with theoretical values that were determined using a modulus of elasticity calculated from the empirical formula in American Concrete Institute (ACI) 349-85.[8] This empirical formula generally gave a higher value for the concrete's modulus than was measured from test specimens. In the following summary of previous test results, theoretical stiffness values were determined using measured moduli as determined from the ASTM standard test. This investigation is concerned with determining the proper values of stiffness to be used in the analysis of Seismic Category I Structures because it is felt that the best estimate of actual material properties should be used when experimental results are compared with theory. The previously reported comparisons between measured and theoretical stiffness do, however, provide information concerning errors that could occur during the design process if material properties have yet to be measured. Table I summarizes the previous results using both the measured and design values for the concrete's modulus.

A. Isolated Shear Walls

The first static tests were performed on single-story isolated shear walls and were reported in Ref. 2. Five walls were tested, two monotonically and three cyclically. These specimens were made with microconcrete and wire-mesh reinforcement. The amount of reinforcement at the interface of the shear wall-base and shear wall-top plate was varied with the amount of moment reinforcement in the form of threaded steel rods located at the ends of the shear wall.

TABLE I

PREVIOUS STATIC TEST RESULTS

	Measured Stiffness Before Cracking (lb/in.) 1	Ultimate[a] Compressive Strength f_c' (ksi)	Theoretical[b] Stiffness Using Measured Modulus (lb/in.) 2	Theoretical[b] Stiffness Using ACI Empirical Modulus (lb/in.) 3	The Ratio of Columns $\frac{2}{1}$	$\frac{3}{1}$	$\frac{2}{3}$
Isolated Shear Walls:							
1	0.78 x 10⁶	4.34	1.60 x 10⁶	2.33 x 10⁶	2.05	2.99	0.69
2	0.79 x 10⁶	5.89	-	2.71 x 10⁶	-	3.43	-
3	1.0 x 10⁶	7.35	1.90 x 10⁶	3.03 x 10⁶	1.90	3.03	0.63
4	1.06 x 10⁶	6.86	-	2.92 x 10⁶	-	2.75	-
5	0.87 x 10⁶	6.31	1.75 x 10⁶	2.80 x 10⁶	2.02	3.22	0.63
1/30-Scale, 1-Story, Diesel Generator Buildings:							
3D-2	0.76 x 10⁶	2.70	2.25 x 10⁶	2.90 x 10⁶	2.96	3.82	0.78
3D-4	1.74 x 10⁶	3.32	4.82 x 10⁶	6.08 x 10⁶	2.77	3.49	0.79
3D-7	0.92 x 10⁶	2.35	2.45 x 10⁶	2.71 x 10⁶	2.66	2.95	0.90
3D-8	0.80 x 10⁶	2.30	2.36 x 10⁶	2.68 x 10⁶	2.95	3.35	0.88
3D-9	1.67 x 10⁶	2.69	4.62 x 10⁶	5.47 x 10⁶	2.77	3.27	0.84
3D-10	1.14 x 10⁶	3.27	-	3.19 x 10⁶	-	2.80	-
3D-11	0.92 x 10⁶	3.09	-	3.11 x 10⁶	-	3.38	-
3D-12	1.23 x 10⁶	2.05	-	2.53 x 10⁶	-	2.06	-
3D-13	0.88 x 10⁶	2.04	-	2.52 x 10⁶	-	2.86	-
3D-19	0.80 x 10⁶	4.70	-	3.83 x 10⁶	-	4.79	-
3D-20	1.08 x 10⁶	4.30	3.22 x 10⁶	3.65 x 10⁶	2.98	3.38	0.88
TRG-1	0.75 x 10⁶	3.77	1.2 x 10⁶	1.3 x 10⁶	1.60	1.73	0.92
TRG-3	4.4 x 10⁶	3.81	3.0 x 10⁶	5.0 x 10⁶	0.68	1.13	0.60
TRG-4	8.5 x 10⁶	4.15	8.4 x 10⁶	9.6 x 10⁶	0.99	1.13	0.88
TRG-5	6.9 x 10⁶	5.03	6.8 x 10⁶	7.1 x 10⁶	0.99	1.03	0.96

[a]The empirical modulus, $E_{c_{ACI}}$, is $57,000\sqrt{f_c'}$, and the measured modulus, E_{c_m}, can be computed by the following formula:

$$E_{c_m} = 57,000\sqrt{f_c'} \left(\frac{\text{Stiffness Col. 2}}{\text{Stiffness Col. 3}}\right)$$

[b]Based on the gross section.

All specimens remained essentially linear up to a load producing an average base shear stress (ABSS) of 200 psi and a principal tensile stress (PTS) of 600 psi or more. The load at first cracking, as predicted from a strength-of-materials approach, agreed very well with the measured cracking strength of the walls and the average split-cylinder tensile strength of 666 psi. Also, when the walls were subjected to repeated load cycles below the first-cracking load, there was no evidence of stiffness degradation or evidence of increase in the area of the hysteresis loop for a given load level. Above the first-cracking load, stiffness degraded and the area of the hysteresis loop increased with increased load and more cycles at a constant load. The ultimate strength of the walls exceeds the provisions for shear capacity as determined by ACI 349-85, 11.10. The measured stiffnesses in the linear region were down by a factor of 1.90 to 2.05 from the calculated uncracked cross-section stiffness, as determined by using a measured modulus.

When normalized to a common modulus of elasticity, these static stiffness values can be compared with those measured indirectly during sine sweep and simulated seismic tests of similar models. At force levels that were 10% of the load required to produce first cracking in the static test, stiffnesses measured during both the sine sweep and simulated seismic tests were reduced considerably from the static tests and even further reduced from the calculated uncracked cross-section value. The "sine-sweep values" and seismic resonant frequency values were reduced on the average by a factor of 2.6 and 2.0 from the calculated uncracked value, respectively. This reduction suggests that stiffness values were down on the average by a factor of 6.95 and 3.85 from the calculated uncracked value, respectively, and down by an average factor of 2.93 and 1.86 from the average measured static value.

B. 1/30-Scale, Single-Story, Diesel Generator Buildings

Eleven 1/30-scale, single-story, diesel generator buildings were statically tested to failure and are reported in Ref. 3. Nine models were tested monotonically, eight in the transverse direction, and one in the longitudinal direction. Two models were tested cyclically, one each in the transverse and longitudinal directions. These specimens were all made with microconcrete and wire-mesh reinforcement. Other than the direction of applied load, the only parameters that were varied in these tests were the amount of cure time each model experienced prior to testing and the embedment length of the reinforcement into the base of the structure.

As with the isolated shear walls, all specimens remained linear up to the load that produced visible cracking. This load produced an ABSS on the order of 200 psi and a PTS on the order of 340 psi. At a given load level below the first-cracking load, the area under the hysteresis loop remained constant when the load was cycled and the stiffness remained constant. Above the cracking load, stiffness was again observed to degrade and the area of the hysteresis loop increased with either increases in load level or with increases in the number of load cycles. The load at first cracking was in good agreement with the value predicted from strength-of-materials and the measured tensile stress of the concrete. Provisions for the shear capacity of the walls from ACI 349-85 were exceeded. Stiffness based on a secant from the origin to half the ultimate load was down by factors ranging from 2.7 to 3.0 when compared with the calculated stiffness based upon an uncracked cross section and a measured modulus.

When similar models were tested dynamically with a 0.5-g's peak acceleration random input, producing an ABSS of 6.3 psi and a PTS of 10.6 psi, the models were again found to behave with resonant frequencies that were a factor of 1.7 to 1.95 below theory, thus suggesting that stiffnesses were down by a factor of 2.9 to 3.8 from the strength-of-materials prediction made using a measured modulus.

It should be noted that the moment of inertia used in the calculated stiffness value considered the entire end wall to contribute to the flexural stiffness of the shear wall, and the modulus of elasticity was based upon the measured values. No effect from cure time or embedment length was observed.

C. TRG-Type Structures

TRG-3 and the two 1/4-scale models of it, TRG-1 and -2, were tested statically and monotonically at low-load levels that produced an ABSS of 28 psi and a PTS of 40 psi on TRG-3 and an ABSS of 53 psi and a PTS of 80 psi on TRG-1 and -2. These tests were repeated several times and were intended to identify the initial stiffness condition of each model while introducing a minimum amount of damage into the test structure. TRG-3 was constructed with conventional concrete and No. 3 rebar and TRG-1 and -2 were made with microconcrete and wire-mesh reinforcement.

TRG-3 showed a measured stiffness up by a factor of 1.47 from the uncracked cross-section stiffness and TRG-1 showed a reduction of 1.60 from the theoretical stiffness. In both cases, the theoretical stiffness was computed with a measured value of E_c. However, the measured modulus for TRG-3 was considerably less than the ACI empirical modulus (2.1×10^6 psi compared with 3.5×10^6). TRG-2 was found to have significant shrinkage cracks, and results from this model were not considered representative. When properly scaled, the static stiffness values for the two models were in good agreement, showing that stiffness can be scaled from microconcrete to conventional concrete in this low-load level region.

When TRG-1 was subjected to a 0.5-g peak acceleration random input, it responded with a stiffness that was down by a factor of 2.6 from theory (as inferred from a resonant frequency that was a factor of 1.6 below theory), even though this excitation produced only 16.3 psi ABSS and 16.6 PTS. Similar stiffness values were obtained during a 0.5-g peak seismic test. TRG-3 responded to a 0.73-g seismic test with a stiffness that was down by a factor of 4.0 from theory at an ABSS of 91 psi and a PTS of 92 psi.

TRG-4 and TRG-5 were tested statically to failure in a cyclic manner. These structures exhibited repeatable linear response with stiffnesses that were almost identical to theory until first-cracking. For TRG-4, first-cracking occurred when an ABSS of 131 psi and a PTS of 171 psi was reached, and for TRG-5, cracking occurred approximately at an ABSS of 167 psi and at a PTS of 227 psi. "Approximately" is used with the TRG-5 value because an unplanned load excursion prevented the actual value from being recorded. The components of stiffness attributable to shear and bending were separated, and these components also agreed with their respective theoretical values. After cracking, the structure again behaved in a linear manner when loaded to levels that did not exceed the peak load during the first-cracking cycle. During these cycles, the stiffness was down by a factor of 2, with the loss occurring equally in each component of the stiffness.

9

IV. TRG-6 MODEL CONSTRUCTION AND MATERIAL PROPERTIES

A primary concern in construction of this model was that it be subjected to a minimum amount of handling once it was built, which would eliminate damage caused by handling as a possible source of any measured reduction in stiffness. To alleviate this concern, the model was constructed in place on the base of the load frame that was to be used in the cyclic testing. The load frame was designed to minimize base deflections. The frame was located in an indoor test facility so that construction, concrete placement, curing, and testing of the model could be performed in a controlled environment.

The reinforcement in both the shear walls and end walls consisted of No. 3 (3/8-in. diam.) rebar with a specified minimum yield strength of 60,000 psi. The bars were spaced at 7.25 in. on center near each face of the wall, providing two layers of reinforcement. As shown in Fig. 1 , a minimum 1.0 in. of cover was provided for all reinforcement. This exceeds the cover requirements of ACI 349-85, 7.7 for interior walls but did not meet the required 1.5 in. cover for exterior walls. Unless otherwise stated, compliance with a section of ACI 349 implies compliance with the same section in ACI 318.[10] The top and bottom slabs were heavily reinforced with two layers of No. 4 rebar spaced at 6 in. on center.

Prior to placing the concrete, 16 Eaton weldable strain gages were attached to the reinforcement at the locations shown in Figs. 2-4. The gages were wrapped with fiberglass tape to prevent damage during compaction and damage caused by moisture.

Next, form work was put into place on top of the load frame base. The entire interior wall forms were made of Plexiglas so that the concrete placement and compaction could be visually monitored in this structurally critical region. The concrete was placed on July 30, 1987. The concrete mixer arrived at 8:10 A.M. and contained 5.5 yards of concrete. Slump from this truck was measured per ASTM C143[10] and found to be 2.25 in. Fourteen gallons of water were added to bring the slump up to 3.75 in. This batch of concrete was used to pour the entire structure. Mechanical vibrators were continually used to compact the concrete. Fourteen standard 6-in.-dia by 12-in.-high concrete cylinders were taken during the middle of this placement, per ASTM standards C172-82[11] and C31-84.[12]

The concrete was specified as minimum 3500-psi ultimate compressive strength. Five and one-half sacks of cement were used per yard of concrete, and the cement was Ideal type 1-2 low alkali. The course aggregate was 0.75-in. maximum, crusher run, Rio Grande river rock and the fine aggregate was No. 4 sand with gradation conforming to ASTM C33-85.[13]

The test cylinders were removed from their forms and were placed in a curing chamber approximately 80 hours after they were poured. They remained in the chamber for the next 38 days. Forms were left on the model until August 29, 30 days after the model was poured. Exposed surfaces (tops of both the top and bottom slab) were kept moist and were covered with tarps during this 30-day period.

|←—18—→|←—24 1/2—→|←—19 1/2—→|←—22 3/4—→|←—20 3/4—→|14 1/2|
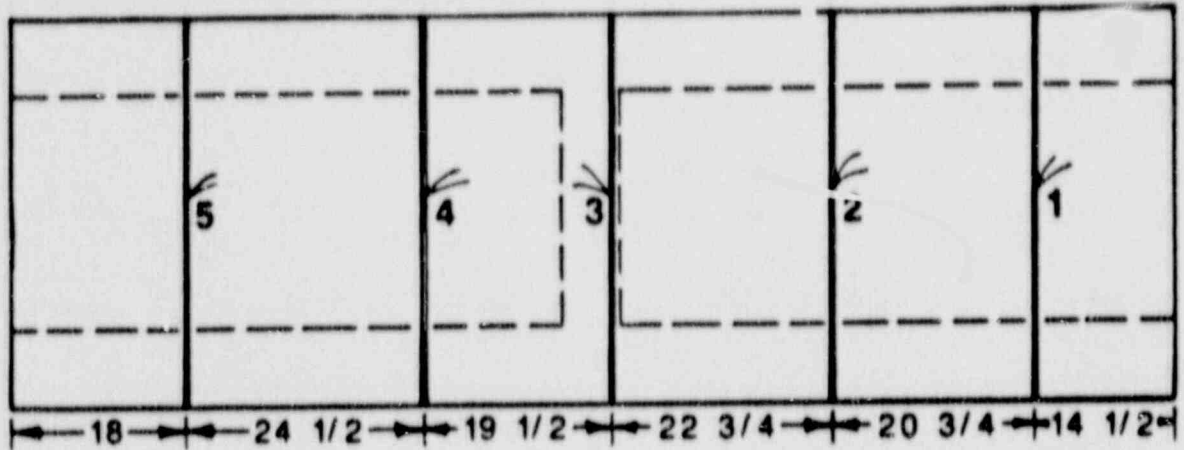
Fig. 2. Strain gage locations in the west end wall.

|←14 1/2→|←—23—→|←—21—→|←—22 1/4—→|←—20 3/4—→|←18 1/2→|
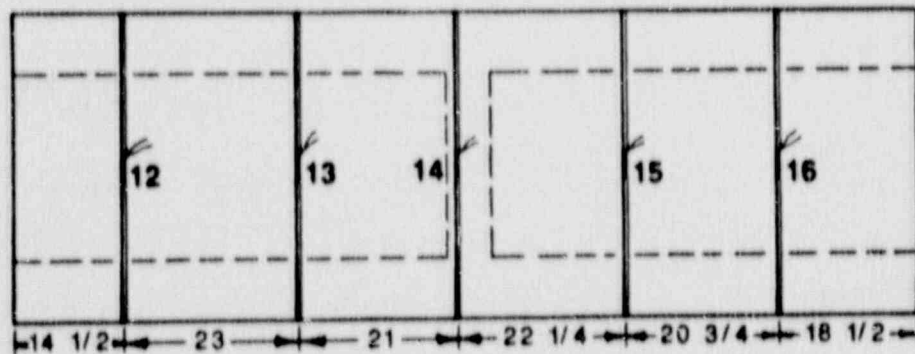
Fig. 3. Strain gage locations in the east end wall.

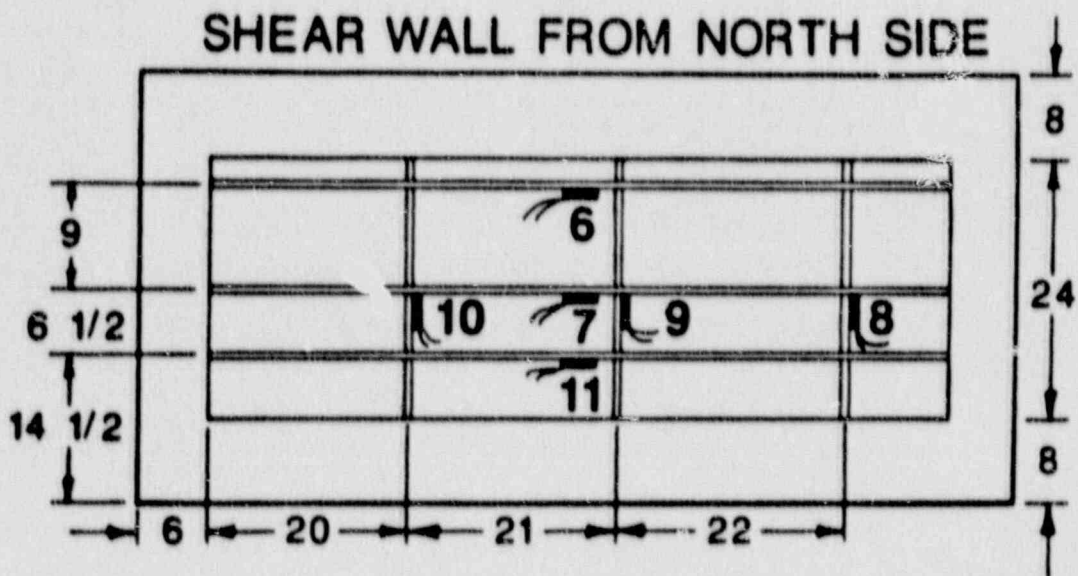## SHEAR WALL FROM NORTH SIDE

Fig. 4. Strain gage locations for the shear wall.

The test cylinders were taken to Albuquerque Testing Laboratories (ATL), where they were tested on September 12, 1987. To avoid damage to the specimens while they were in transit to Albuquerque, a foam-lined transportation box was constructed and foam was placed between each of the individual cylinders. Tests included ultimate compressive strength (ASTM C39-84),[14] modulus of elasticity (ASTM C469-83),[15] split-cylinder tensile strength (ASTM C496-85),[16] and density. Six specimens were tested for ultimate compressive strength and modulus of elasticity, and four specimens were tested for tensile strength. The specimens were weighed to the nearest 0.01-lb. Results of the tests are summarized in Table II and the report from the testing lab is included as Appendix A. Errors were made by ATL in computing the modulus of elasticity; hence, the plots in Appendix A have a line with the slope equal to the modulus computed by Los Alamos drawn tangent to the measured data. Also drawn on these plots for comparison is a line from the origin with a slope equal to that modulus reported by ATL.

TABLE II
MEASURED MATERIAL PROPERTIES

	Density (w) (lb/ft^3)	Ultimate Compressive Strength (psi) [a]	Tensile Strength (psi) [b]	Modulus of Elasticity (psi) [c]	$57,000\sqrt{f'_c}$ (psi) [d]	$33w^{3/2}\sqrt{f'_c}$ (psi) [d]
Average Truck 1	142	4690	380	3.45×10^6	3.90×10^6	3.82×10^6
Minimum	141	4170	355	4.29×10^6	3.68×10^6	3.58×10^6
Maximum	142	4880	420	2.98×10^6	3.98×10^6	3.90×10^6

[a] Measured on 6-in. diam x 12-in. specimens per ASTM C39-84.
[b] Measured on 6-in. diam x 12-in. specimens per ASTM C496-85.
[c] Measured on 6-in. diam x 12-in. specimens per ASTM C469-83.
[d] Modulus of elasticity determined per ACI 349-85,8.5.1.

On August 24-25, 1987, Luke Snell, a faculty member at Southern Illinois University and an experienced independent consultant in the field of ultrasonic testing of reinforced concrete structures, performed an ultrasonic test on TRG-6. He began by visually inspecting the model for surface cracks and voids; none were found. Next, he calibrated his testing equipment with a standard steel specimen and proceeded to test the 6-in.-diam by 12-in.-long test specimens. The test consisted of applying an audio pulse to the end of the specimen and measuring the time required for that pulse to travel over the distance of the specimen. From this information, the speed of sound in the concrete can be estimated and defects in the concrete can be identified when the speed is altered because the sound wave cannot travel across a void but, rather, must go around it. The cylinders from this mix showed no significant difference in pulse speed. Pulse velocities were determined at 34 locations on the model, and the results are summarized in Table III. From these results Mr. Snell concluded that the model showed no signs of defects and that material properties determined from the cylinder test specimens should be indicative of the properties of the TRG-6 structure. Mr. Snell's test data is included as Appendix B.

Other investigations (Ref. 17) have correlated the speed of sound in concrete to the static modulus of elasticity. However, these investigations do not specify the type of static modulus, that is, initial tangent, secant to 40% of ultimate, etc. A similar correlation, made by interpolating between the data points in Ref. 17 with the results of Mr. Snell's test, would yield an average modulus of 3.56×10^6 psi for the TRG-6 structure.

TABLE III
ULTRASONIC TESTING OF TRG-6

	Cylinders	Shear Wall	West End Wall	East End Wall	Top	Base
Average Pulse Velocity (ft/s)	14,100	13,900	13,400	13,700	13,100	-

V. MODAL TESTING AND RESULTS

The first test performed on the TRG-6 structure was a low-load level experimental modal analysis. This test was used to characterize the initial stiffness of the model without introducing damage and to demonstrate that the dynamic properties of the structure could be accurately measured at very low-load levels. The test configuration consisted of simulating free boundary conditions by supporting the model with five air bearings. Free boundary conditions were chosen because they can be most accurately compared with analytical results from finite element analysis (FEA).

A 300-lb peak force shaker was attached to the Northwest end wall 4 in. from the bottom. A transducer, located between the shaker's stinger and the model, measured force as the input quantity. A random excitation signal with a uniform power spectral density between 0 and 250 Hz was used to drive the shaker. Acceleration response was measured in three orthogonal directions at 76 points on the structure. The measurement points are shown in Fig. 5. The excitation was applied at Pt. 2 in the Y-direction.
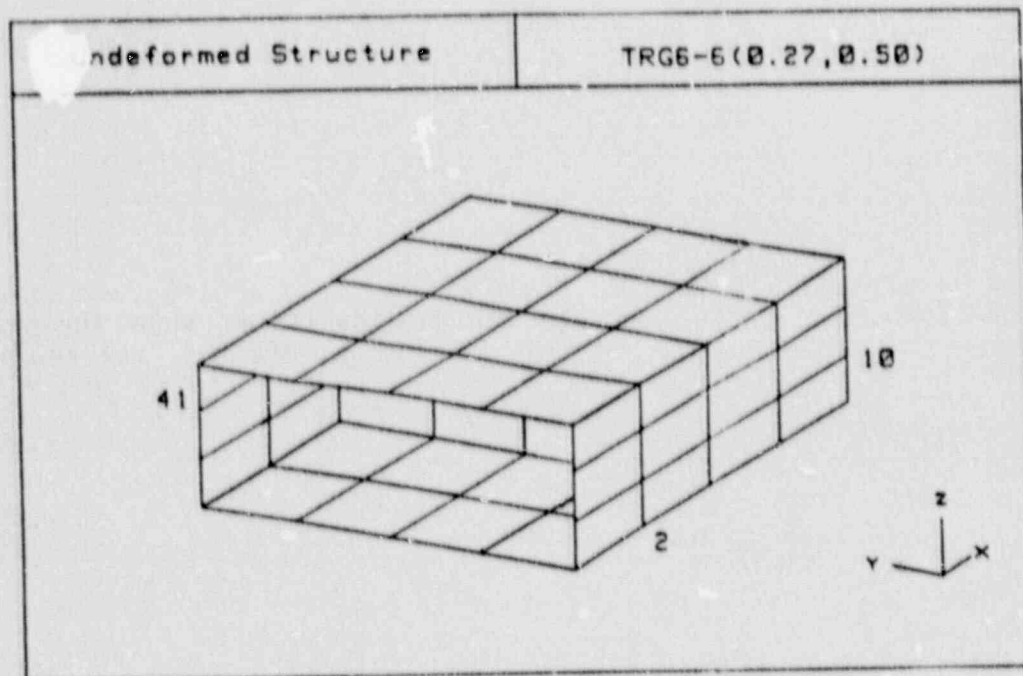

Fig. 5. Acceleration measurement points for the experimental modal analysis. Data were taken at each line intersection (76 points).

The force input and acceleration responses were recorded, transformed into the frequency domain, and analyzed with a commercially available experimental modal analysis software package. Coherence functions showed that the 300-lb shaker had only enough force capacity to excite the structure at its resonant frequencies. The frequency domain representation of the input and response was used to calculate a set of frequency response functions. Typical examples of the frequency response functions are shown in Figs. 6 and 7 and correspond to responses measured at Points 41 and 10 in the Y and Z direction, respectively. From these plots, resonant frequencies can be identified from zero crossings in the real portion that corresponds to peaks in the imaginary portion. Five resonant frequencies and corresponding mode shapes were experimentally identified between 0 and 250 Hz.
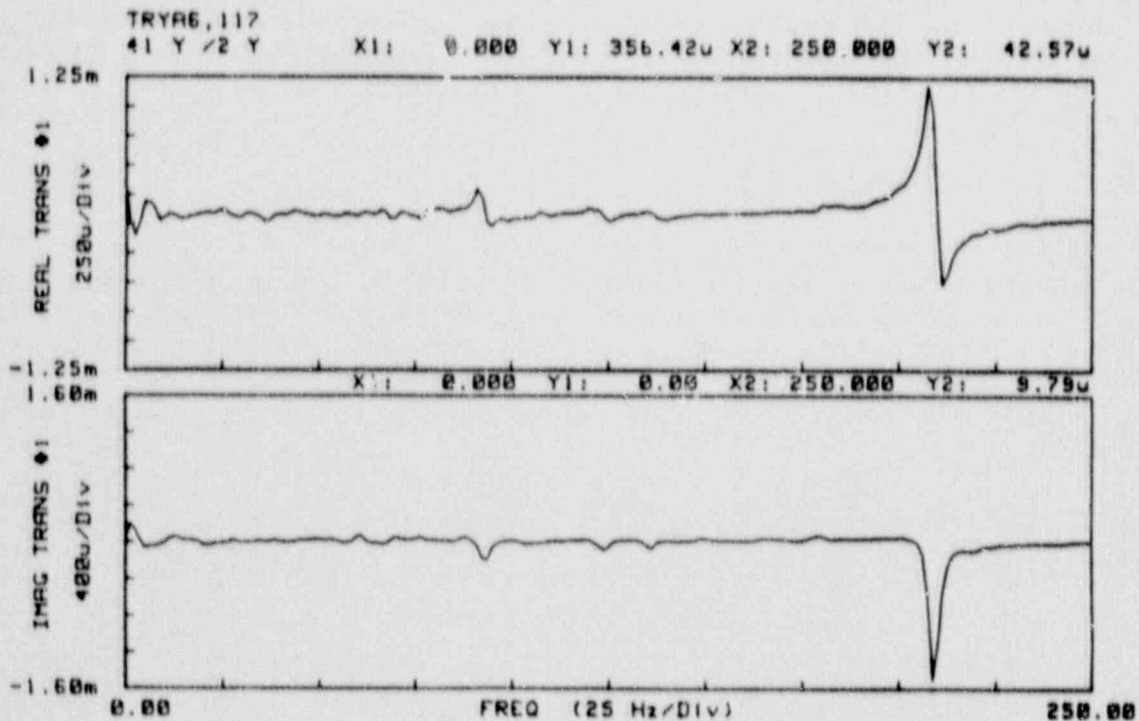

Fig. 6. Frequency response function Pt. 41Y/2Y.

A finite element analytical modal analysis was also run for comparison with the experimental modal analysis. Half the structure was modeled with free boundary conditions at the base and appropriate boundary conditions applied along the plane of symmetry so that all modes below 250 Hz could be identified. The undeformed mesh and the first three modes are shown in Fig. 8 and a direct comparison between an experimental and FEA mode is shown in Fig. 9. Average measured material properties were used in these calculations (modulus of elasticity of concrete = 3.45×10^6 psi). A comparison of the corresponding analytical and experimental resonant frequencies is presented in Table IV. The mode that showed up in the FEA but did not show up in the experimental modal analysis was not sufficiently excited by the amplitude and direction of the applied excitation. A larger shaker and/or change in the direction and location of excitation would have identified these modes. However, it was felt the objectives of the modal testing were accomplished with the one excitation location.
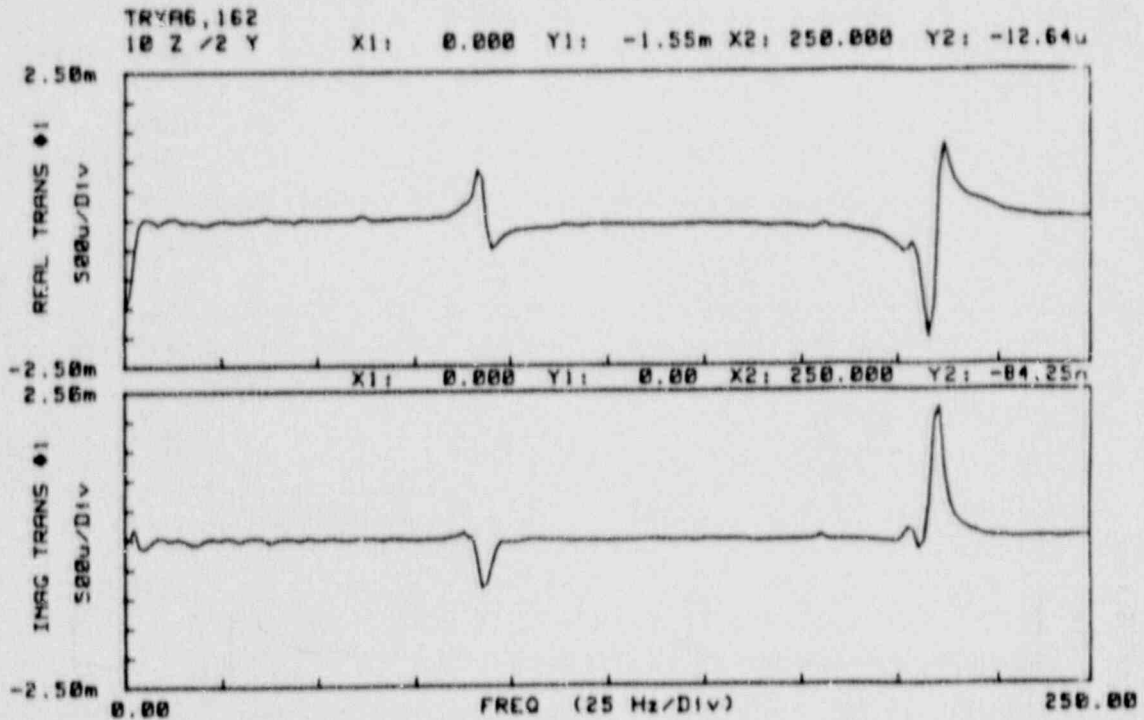
14

Fig. 7. Frequency response function Pt. 1OZ/2Y.

Based on the fundamental frequency and noting that

$$\left(\frac{f_{measured}}{f_{calculated}}\right)^2 = \frac{k_{measured}}{k_{calculated}}$$

where f is frequency, and K is stiffness, a comparison can be made between the low-load level dynamic stiffness and the calculated stiffness from FEA. The measured stiffness as a percentage of theoretical is summarized for various moduli values in Table V.

Finally, by adjusting the modulus in the finite element analysis so that the fundamental frequencies match the measured fundamental frequency, one can indirectly estimate the actual modulus of the concrete in the TRG-6 model. The value of E_c that made the FEA agree with the measured fundamental frequency was 3.53×10^6 psi, close to the value that was determined from the material testing.

The results of the experimental modal analysis show good agreement with the analytical modal analyses and seem to verify that the initial stiffness was very close to theoretical. When examining the results, it should be remembered that, if nonlinearities due to cracking or voids did exist, they would produce excitation amplitude-dependent response in the structure and, at the load levels used in this test, the effects of these nonlinearities might not appear.
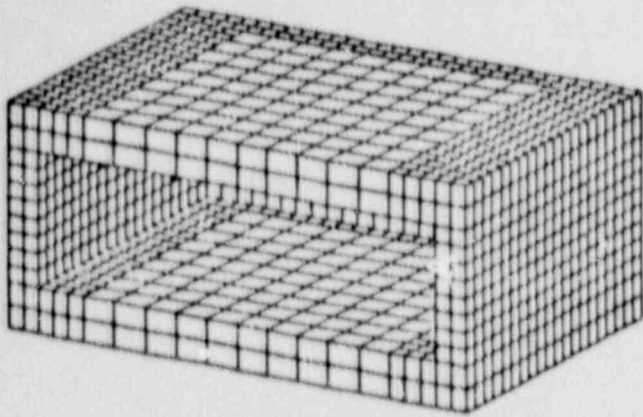
TRG6 UNDEFORMED MESH
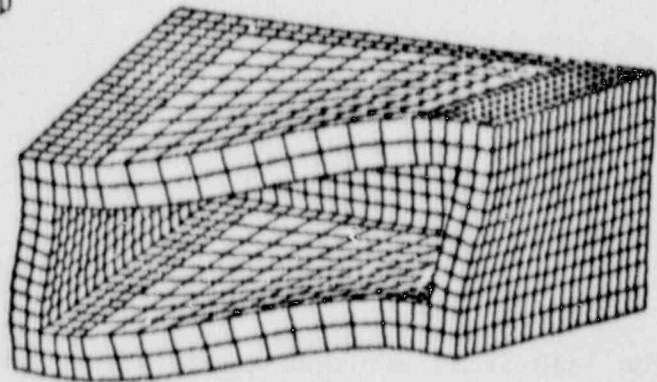
MODE 1, ASYMM. B.C.
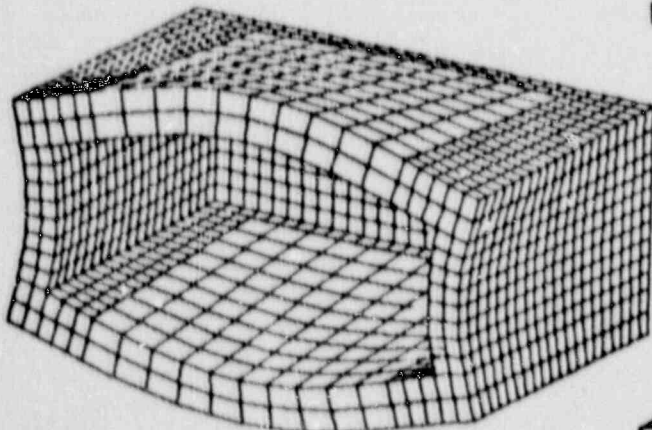
MODE 2, ASYMM. B.C.

MODE 3, SYMM. B.C.

Fig. 8. The first three modes identified
by the finite element analysis.

16

The lifting of the TRG-6 structure for air-bearing placement during the modal analysis was the only handling of the structure during the entire testing sequence.

VI. STATIC TEST SETUP AND LOAD SEQUENCE

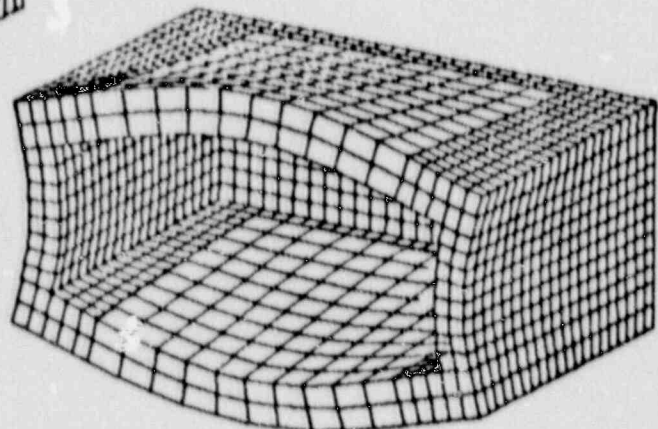After the modal testing was complete, the structure was bolted to the load frame base (Fig. 1). Two 2-in.-thick steel plates were placed on top of the base, grouted level, and thirty-six 1.25-in.-diam steel bolts were placed through the plates in an attempt to obtain a fixed-base boundary condition. The bolts were torqued to 400 ft-lb. Next, the two 6-in.-thick steel plates (Fig. 1) were placed on top of the model, grouted level, and held in place by thirty-six 1.25-in.-diam steel bolts torqued to 400 ft-lb. Because the load was to be applied by a force acting on the bottom 6-in.-thick steel plate, the connection of these steel plates to the concrete slab was designed to provide a friction connection and to produce a distributed load over the top of the structure. This type of loading would be more indicative of that introduced by a seismic event.

The load frame was then assembled around the model and an instrumentation frame was also assembled around the model and independent from the load frame. Twenty-four Ono-Sokki EG-233 displacement transducers were placed on the model and on the instrumentation frame (Fig. 10). Ten gages were mounted on the model itself, providing relative displacement readings that were independent of a rigid body rotation and translation. Of these ten, eight were located on the shear wall and were used to obtain the readings necessary to separate shear and bending components of displacement. Overall structural deformations, including rigid body motion, were monitored with the remaining 14 gages attached to the load frame. These external gages were also used to measure torsional motion, sliding shear at the base of the structure, and the relative displacement between the steel plates on top of the structure and the top concrete slab. Two dial indicators were used to measure the displacement of the bottom steel plate relative to the top concrete slab. These gages were used to give an indication that a friction connection was obtained.

An ENERPAC hydraulic actuator was used to load the structure, and force input was monitored with a load cell located between the actuator and the steel plate. At specified load increments, the strain gages, displacement transducers, and load cell were scanned with an HP 3497A data scanner and were recorded onto floppy disks by an HP 87 computer. After some initial low-level tests to check out the instrumentation, the load history shown in Figs. 11 and 12 was followed until the structure cracked. Each integer on the horizontal axis in Figs. 11 and 12 represents a point at which the data were scanned. In previous tests of our microconcrete structures, it was assumed that repeated cycling at low-load levels would not degrade the structure; thus all of the microconcrete structures tested dynamically were characterized by exciting them with narrow-frequency-band random signals and by using the transfer function method to obtain their natural frequencies. The assumption was made that numerous cycles below an "additional damage" threshold would not degrade the structural stiffness. In an attempt to verify this assumption, at three points in the load history, the structure was cycled numerous times to see if
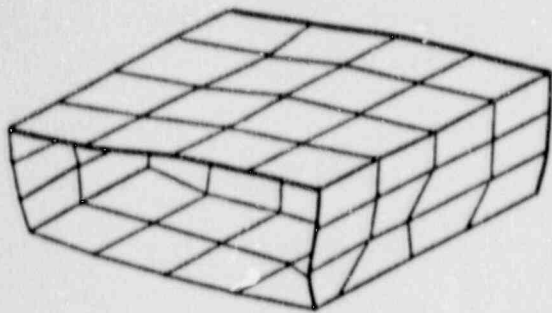
MODE 1
EXPERIMENTALLY
DETERMINED
Freq. = 92.9 Hz
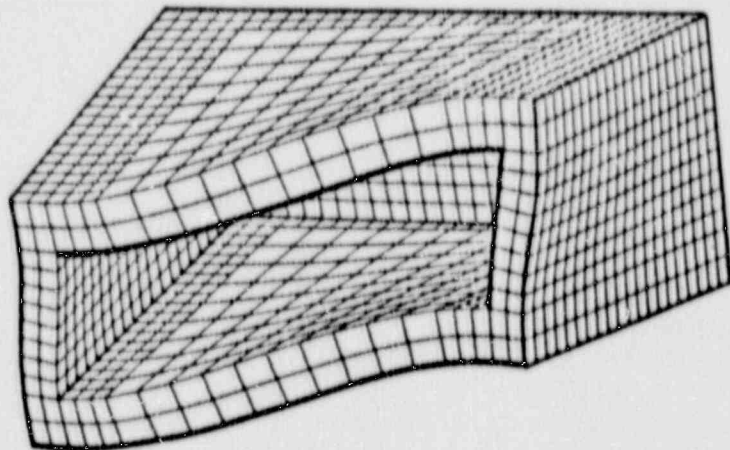
MODE 1
DETERMINED FROM FINITE
ELEMENT ANALYSIS
F = 91.8 Hz

Fig. 9. A comparison of the fundamental mode identiried by
the experimental modal analysis with the fundamental
mode identified by the finite element analysis.

TABLE IV

COMPARISON OF EXPERIMENTAL AND
ANALYTICAL MODAL ANALYSIS
RESULTS
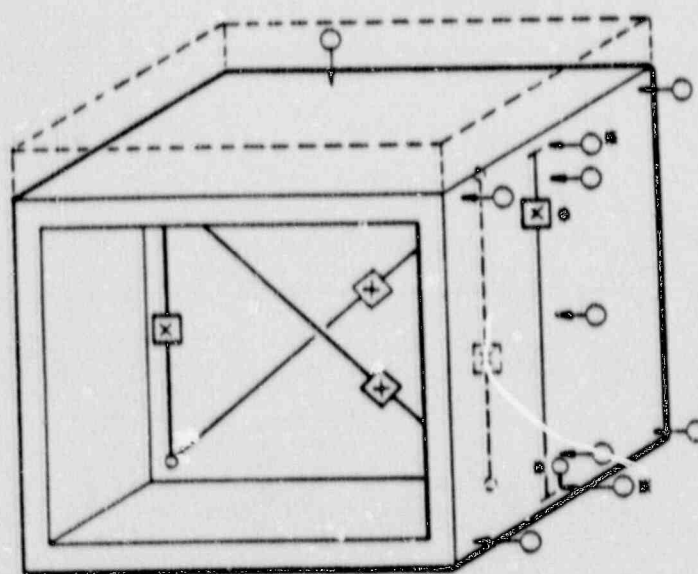
Mode	Experimental	FEA with Measured Modulus
1	92.9	91.8
2	123.4	125.1
3	136.4	134.9
4	179.2	172.6
5	208.8	196.2
6		206.1

---

* Not identified.

TABLE V

THE RATIO OF THE MEASURED FREQUENCY-INFERRED STIFFNESS TO THE STIFFNESS CALCULATED BY FINITE ELEMENT ANALYSIS USING VARIOUS VALUES OF E_C

	Measured E_C	$E_C = 57,000\sqrt{f_c}$	$E_C = 33w^{3/2}\sqrt{f_c}$
K_m/K_t	1.04	0.92	0.98

— RELATIVE DISPLACEMENT

— DISPLACEMENT, FIXED REFERENCE

□ FOUR GAGES CORRESPONDING TO THESE ON THE OTHER END

× FOUR GAGES CORRESPONDING TO THESE ON THE OTHER SIDE OF THE SHEAR WALL

Fig. 10. Location of the displacement transducers for static testing.

stiffness would degrade. During these repeated cycles, only the peak displacements and zero load displacements were measured. The complete load reversals shown in this load history were intended to represent the cyclic forces induced in a Seismic Category I Structure during seismic excitation. The breaks in the load history at the end of a cycle were the result of zeroing the hydraulic actuator before the start of the next cycle. These discontinuities were accounted for in the final data reduction.
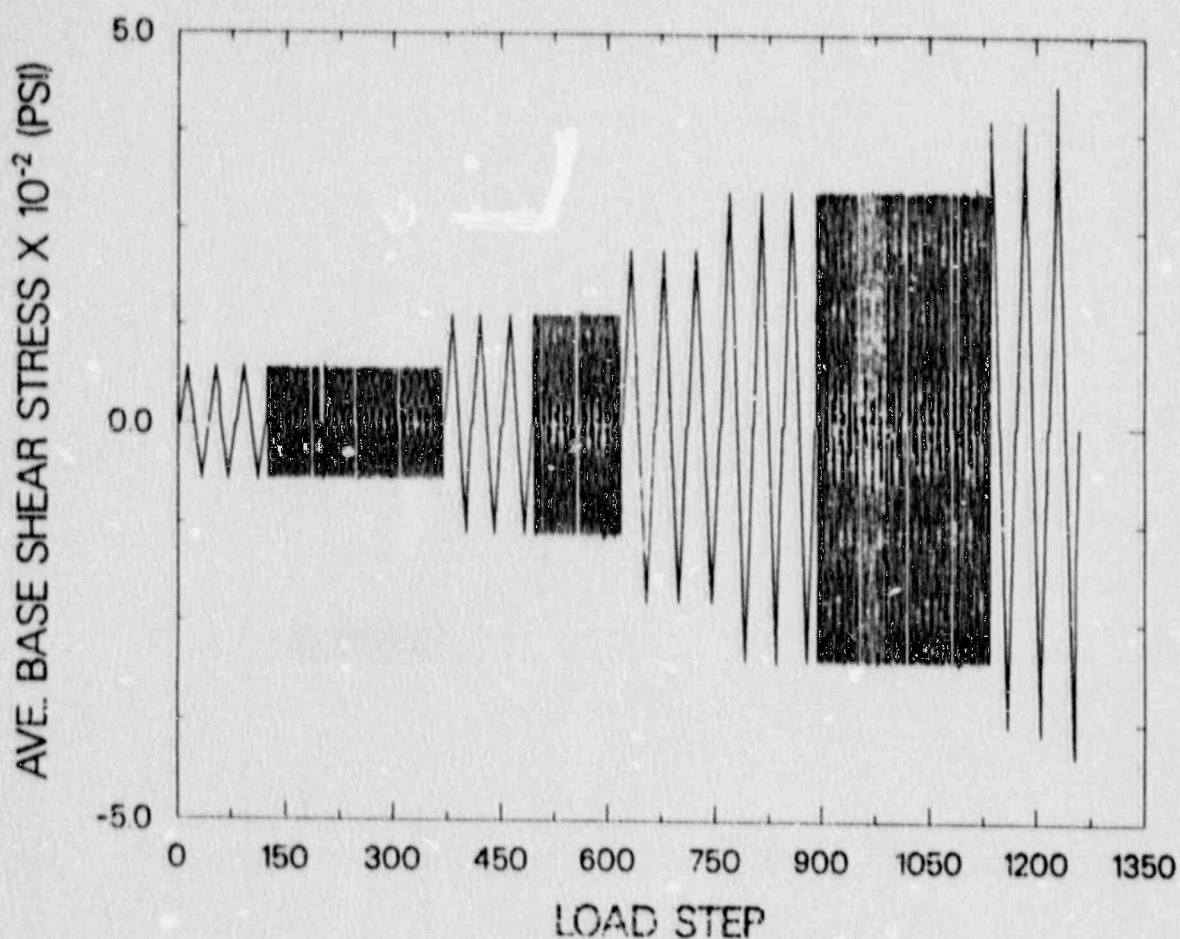
19

Fig. 11.   Average base shear stress
versus load step history.

The load cycling began with three 50-psi ABSS cycles followed by sixty 50-psi peak-to-peak cycles. Next, three 100-psi cycles were performed, followed by thirty 100-psi peak-to-peak cycles. This was followed by three 150-psi cycles, three 200-psi cycles, and fifty-nine 200-psi peak-to-peak cycles. Finally, three cycles were done at 261-psi peak. Two-hundred sixty-one psi was chosen because of an overload that occurred during the sixtieth 200-psi peak-to-peak cycle. For 200 psi and up, the control of the pump for the actuator is very sensitive.

VII. RESULTS

The displacements that occurred during the lower-load cycles (50-psi and 100-psi ABSS) were expected to be and were found to be near the resolution of the relative displacement measurement system. The vertical relative displacement gages that measured deformations over a 16-in. gage length, gave readings that
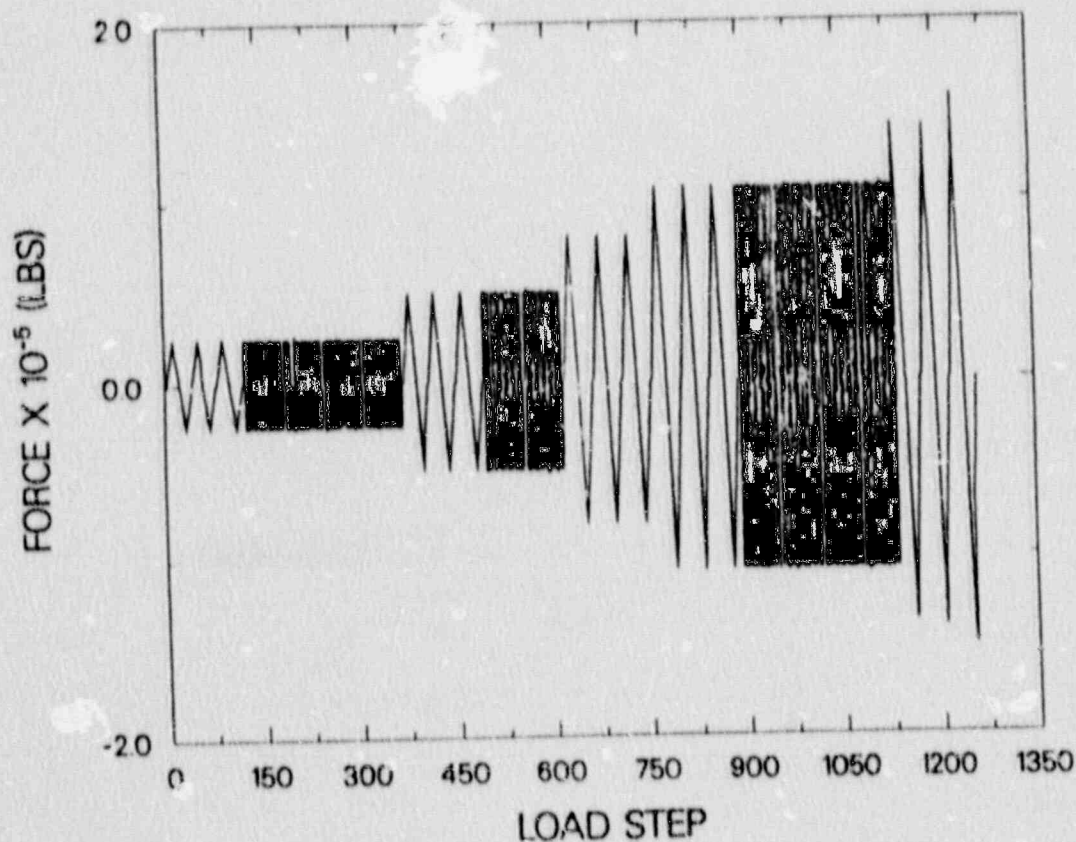
20

Fig. 12.   Force versus load step history.

were at or near the gage's least count. These gages attempt to measure be____ deformations that are calculated to be 2 orders of magnitude lower than s_ear deformation in this structure. Because of these very small bending deformations, the stiffness values were based upon the diagonal relative displacement readings, and these displacements were considered accurate only when the diagonal gages were being compressed. The accuracy of the measuring system generally depends upon the Ono-Sokki return spring overcoming any friction when the gage is in tension. As with previous tests on TRG-type structures, the displacement values determined from the diagonal gage readings represent the displacements at the end of these gages relative to the bottom end of these gages. The displacement field over this region may be nonhomogeneous; hence, the displacements computed in this manner represent an average value for the wall. The method for computing the horizontal displacements is illustrated in Fig. 13 and, with the instrumentation used in this test, theoretically, four values of horizontal displacement could be determined and averaged. However, only two of the diagonal gages gave consistent readings. Because the vertical relative displacement gages were not giving significant readings &RB in Fig. 13 was taken as zero in the data reduction. Figures 14-18 show the horizontal component of displacement, as determined from one of the diagonal gage readings

21
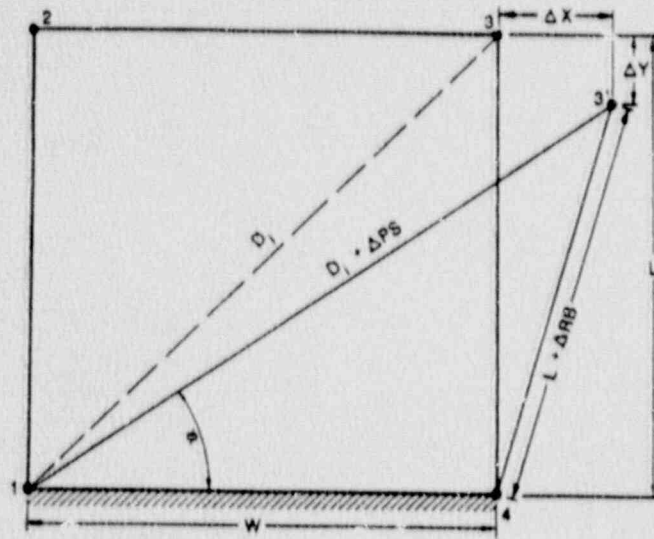
$$\Delta X = (D_1 + \Delta PS) \cos\phi - W$$

$$\Delta Y = (D_1 + \Delta PS) \sin\phi - L$$

$$\phi = \cos^{-1}\left[\frac{W^2 + (D_1 + \Delta PS)^2 - (L + \Delta RB)^2}{2\,W(D_1 + \Delta PS)}\right]$$

ΔPS = DIAGONAL DISPLACEMENT GAGE READING
ΔRB = VERTICAL DISPLACEMENT GAGE READING

Fig. 13. Method used to calculate horizontal displacements from interior relative displacement gages.
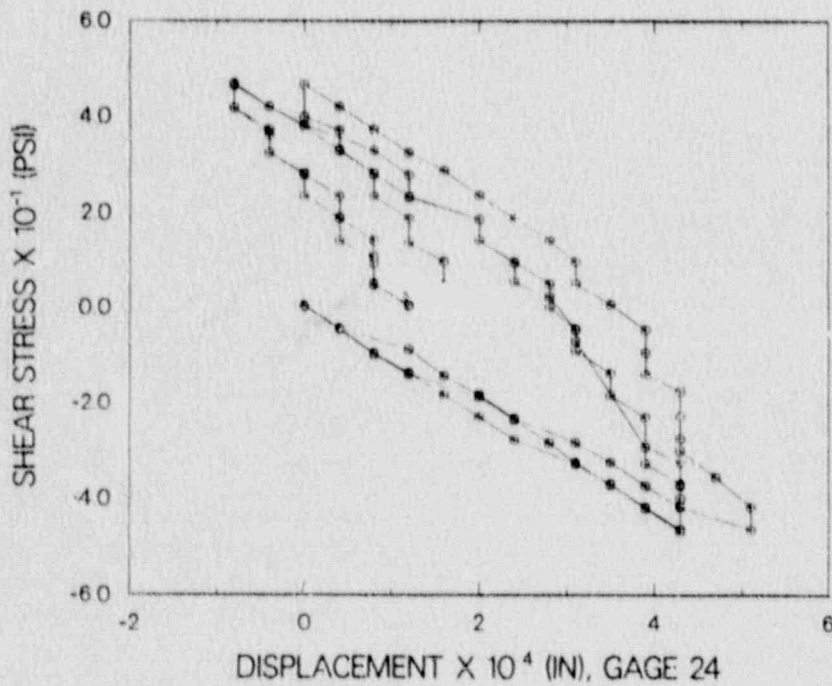

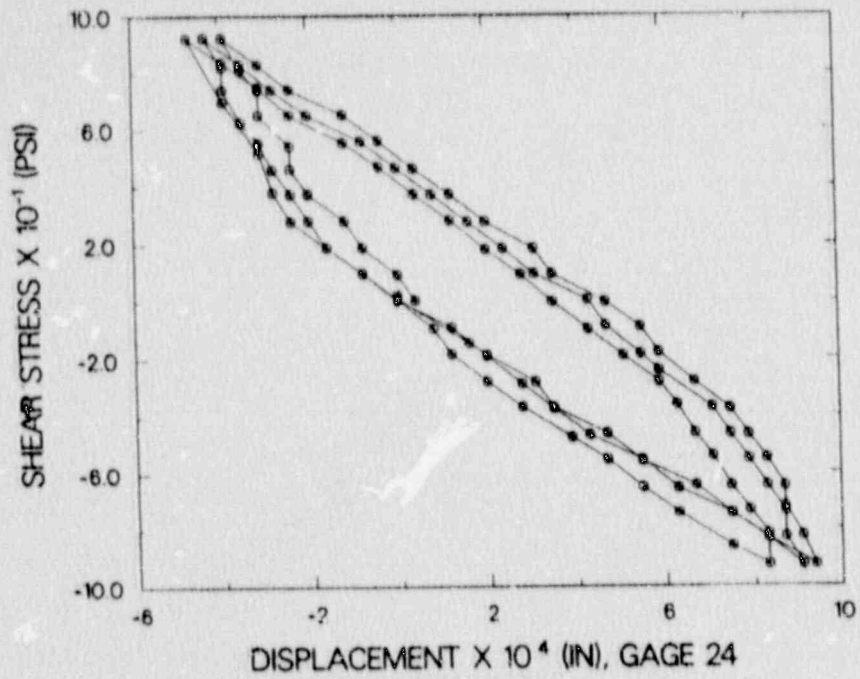Fig. 14. Horizontal displacements from Gage 24, 50-psi ABSS cycles.

Fig. 15. Horizontal displacements from
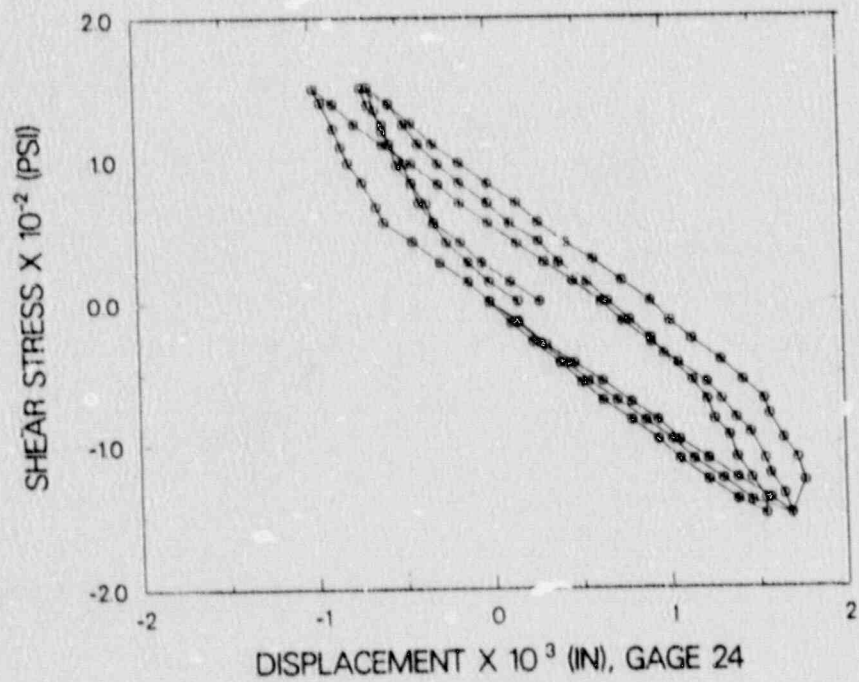Gage 24, 100-psi ABSS cycles.

Fig. 16. Horizontal displacements from
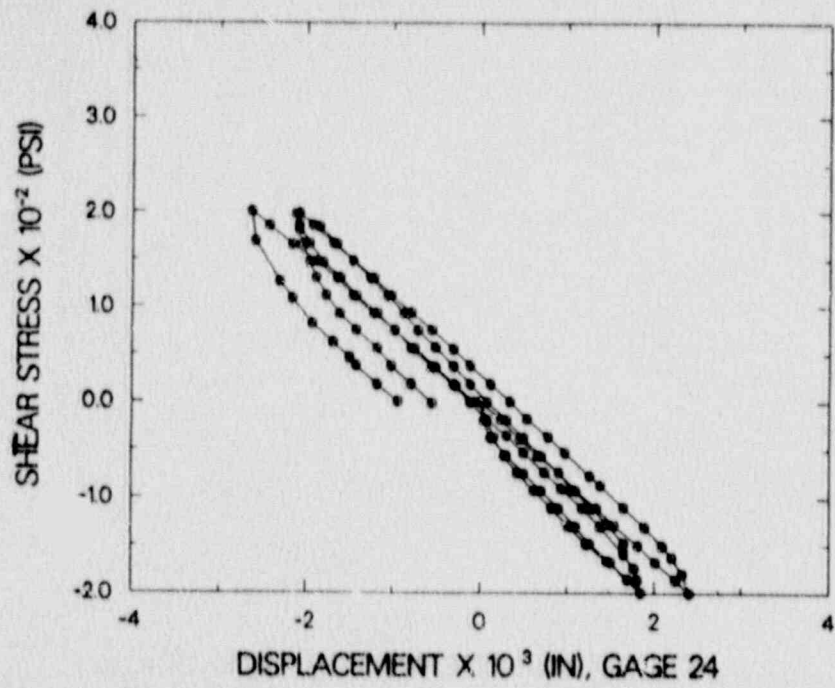Gage 24, 150-psi ABSS cycles.

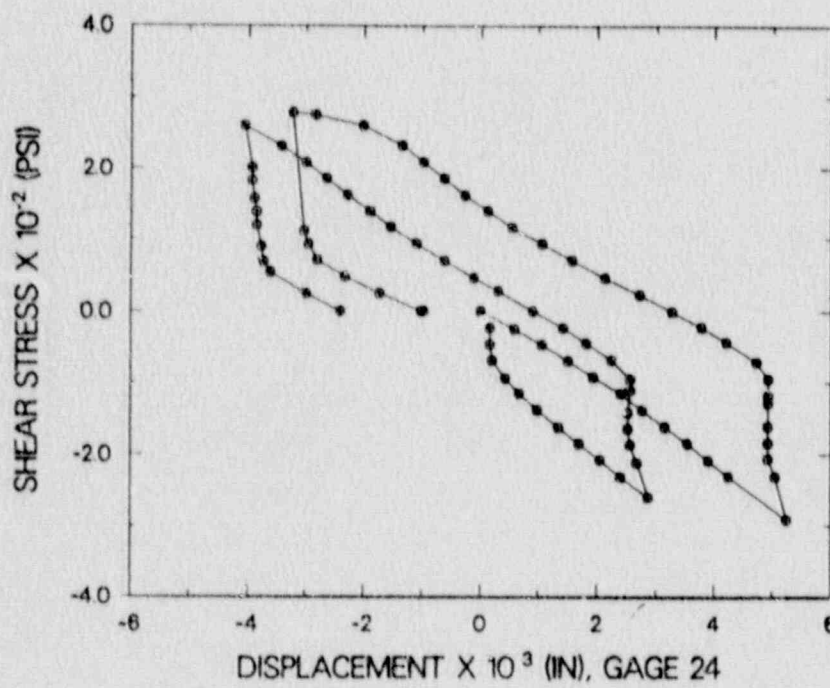Fig. 17. Horizontal displacements from Gage 24, 200-psi ABSS cycles.

Fig. 18. Horizontal displacements from Gage 24, 261-psi ABSS cycles.

24

(Gage 24) for the 50-psi, 100-psi, 150-psi, and 200-psi ABSS cycles, respectively. Gage 24 appeared to give the most reliable readings of the four diagonal gages.

During the 50-psi, 100-psi, and the first 150-psi ABSS cycle, the measured data indicated an average stiffness of 58.2 x 10⁶ lb/in. The structure cracked during the second 150-psi cycle at an ABSS between 140 and 150 psi. Cracking was identified by the significant jump in the strains measured on the vertical reinforcement in the shear wall, as well as by visual inspection of the shear wall. Figure 19 shows the strain readings for Gage 9 (see Fig. 3) during the last 15 peak-to-peak cycles at 100-psi ABSS, the three 150-psi cycles, and the three 200-psi cycles. After the structure cracked, the stiffness reduced to 44.5 x 10⁶ lb/in. during the 200-psi cycles and reduced further to an average value of 35.9 x 10⁶ psi during the 261-psi ABSS cycles. At this point, the capacity of the hydraulic load pump in tension appears to have been reached.

The peak-to-peak cycles at 50 psi and 100 psi showed repeatable response and no deterioration in stiffness. These cycles can be seen in Figs. 20-21. Repeatable response was again observed during the 200-psi peak-to-peak cycles, but at a reduced stiffness. The 200-psi peak-to-peak cycles are shown in Fig. 22. Damage during the 261-psi overshoot during the last 200-psi peak-to-peak cycle can be identified in Fig. 23 by the distinct change in slope that occurred at the end of the cycles.
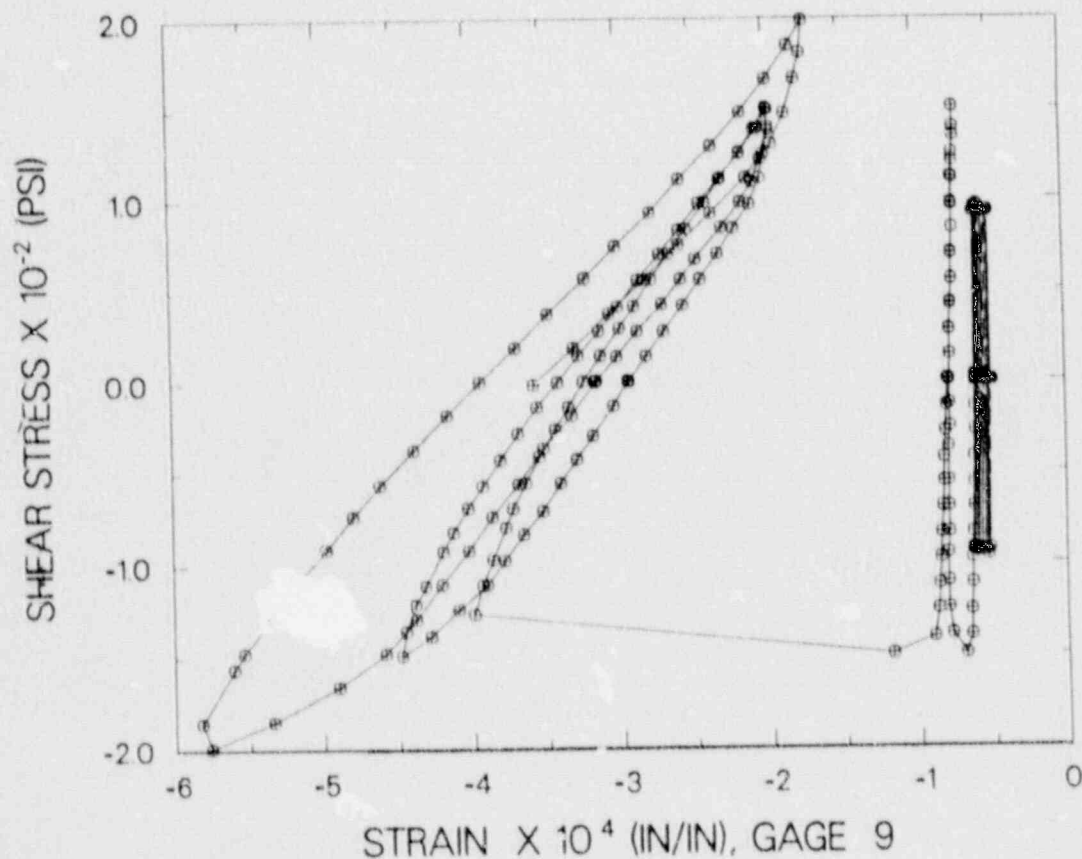
Fig. 19. The onset of cracking as determined from Strain Gage 9.

Fig. 20. Horizontal displacements from Gage 24,
50-psi ABSS peak-to-peak cycles.
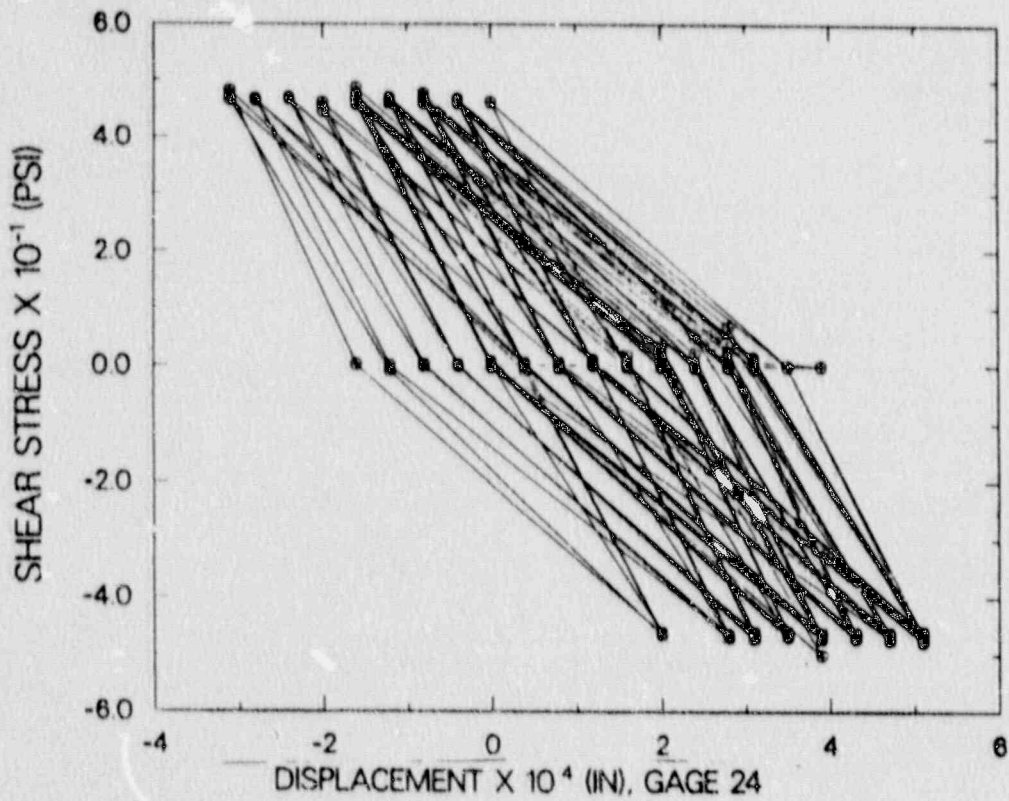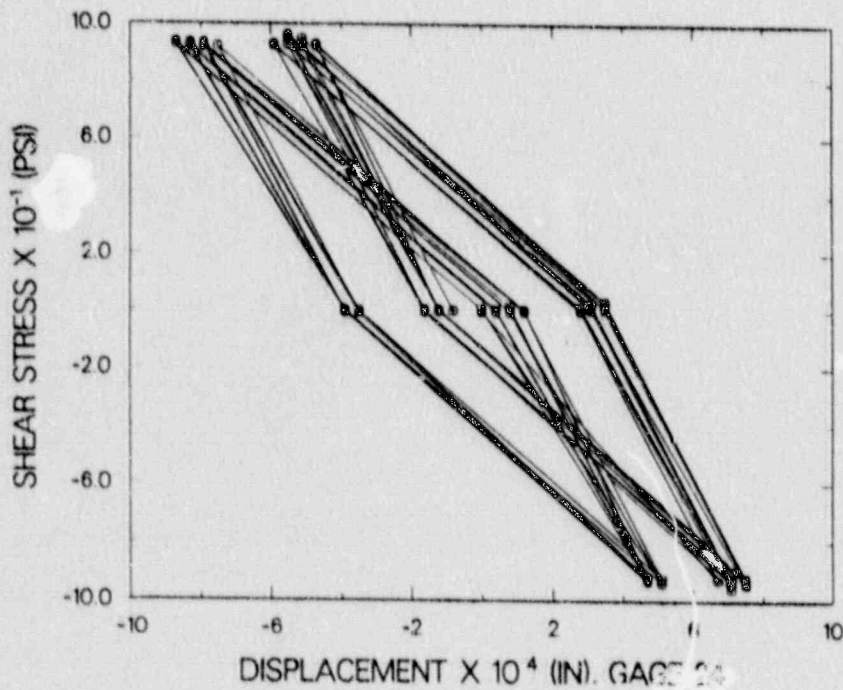

Fig. 21. Horizontal displacements from Gage 24,
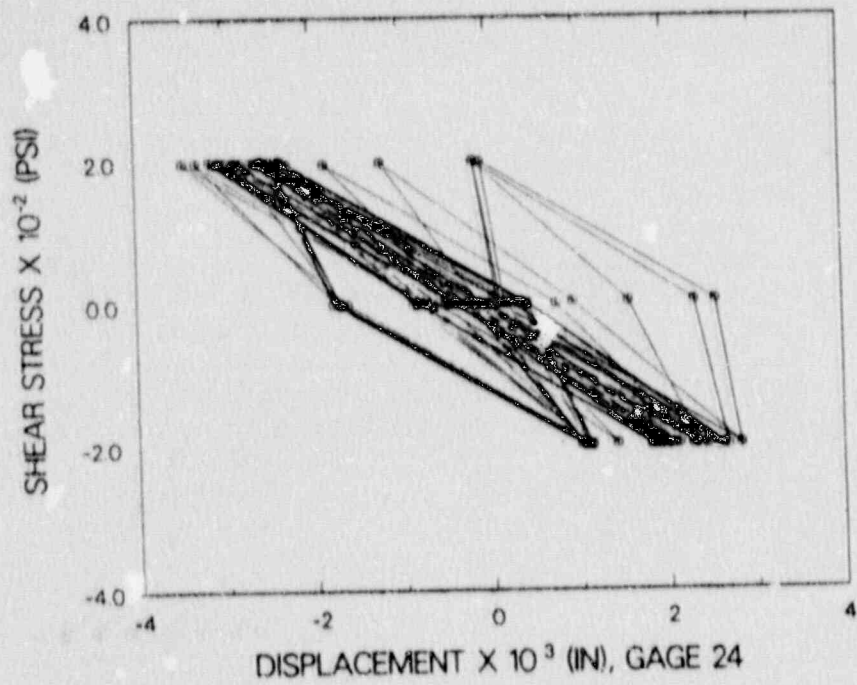100-psi ABSS peak-to-peak cycles.

Fig. 22. Horizontal displacements from Gage 24, first forty-five 200-psi ABSS peak-to-peak cycles.
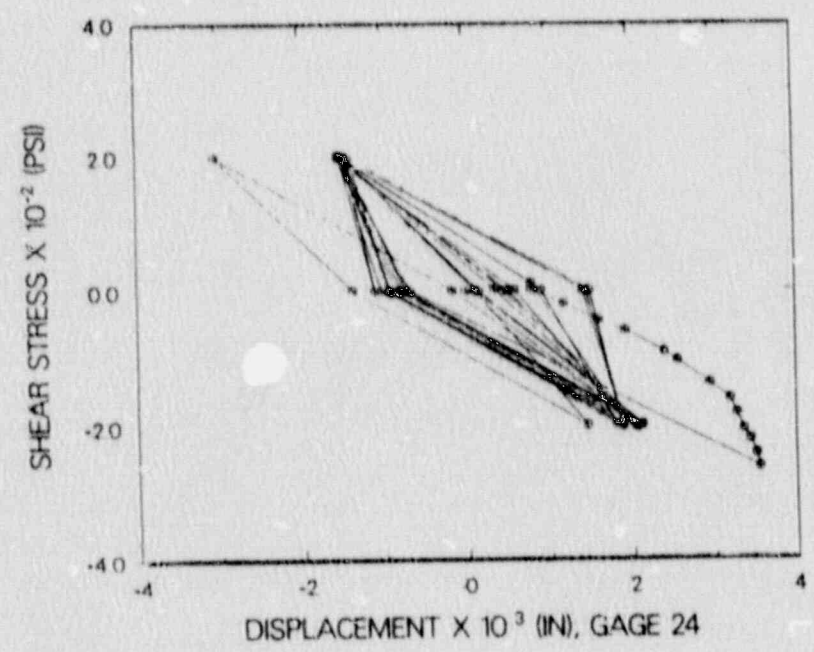

Fig. 23. Horizontal displacements from Gage 24, the last fourteen 200-psi ABSS peak-to-peak fourteen cycles and the 261-psi overshoot.

27

Prior to cracking, TRG-6 responded with a stiffness that was about 20% higher than the strength-of-materials prediction that uses only the shear wall as being effective in carrying the shear. This value would be about 10-12% higher than a 3-D finite element analysis would predict. These differences indicate that the end walls are partially effective in carrying the shear. The stiffness values measured during the static testing were not considered unreasonable, if the magnitudes of the displacements being measured are considered (< 5 mils). Conclusions about the effectiveness of the end walls in bending can only be implied from the displacement measurements because the bending deformations are so small as to be immeasurable with the displacement gages. However, a strength-of-materials calculation indicates that a peak strain of about 8 microstrain would be recorded in the end-wall strain gages for the 100-psi cycle. Figures 24-28 show the strains recorded in the rebar across the east end wall are about this value and are remarkably uniform. Such agreement and uniformity indicate the end walls are nearly fully effective in bending.
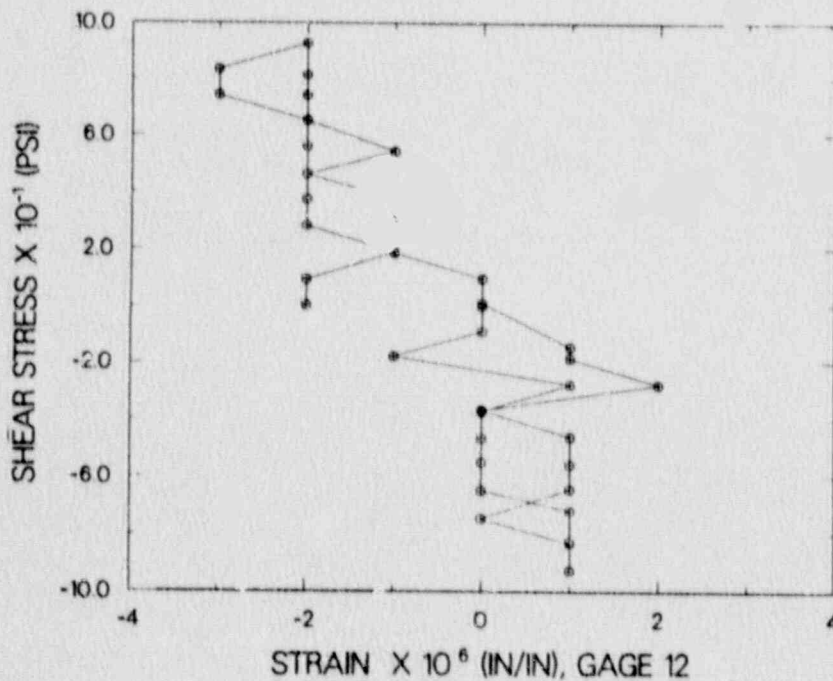
Fig. 24. Vertical strain in Gage 12,
second 100-psi ABSS cycle.

Analytical stiffness values, based upon these relative displacement readings, were determined from Castigliano's Theorem. By examining the free-body diagram in Fig. 29, the expression for internal strain energy stored in the structure between the section A-A and B-B can be written as

$$U = \int_0^L \frac{(M + Px + \delta x)^2}{2EI} \, dx + \int_0^L \frac{(P + \delta)^2}{2 A_e G} \, dx \, , \tag{[1]}$$

28
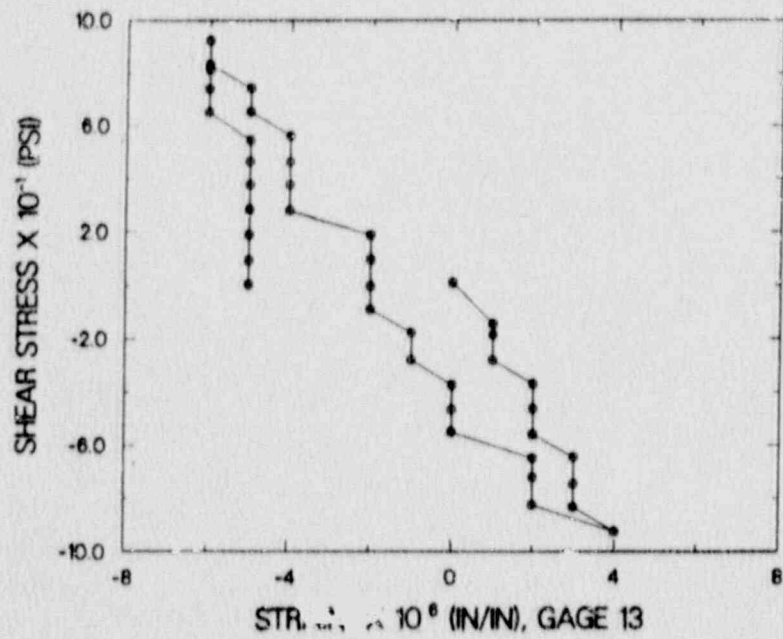
Fig. 25. Vertical strain in Gage 13, second 100-psi ABSS cycle.
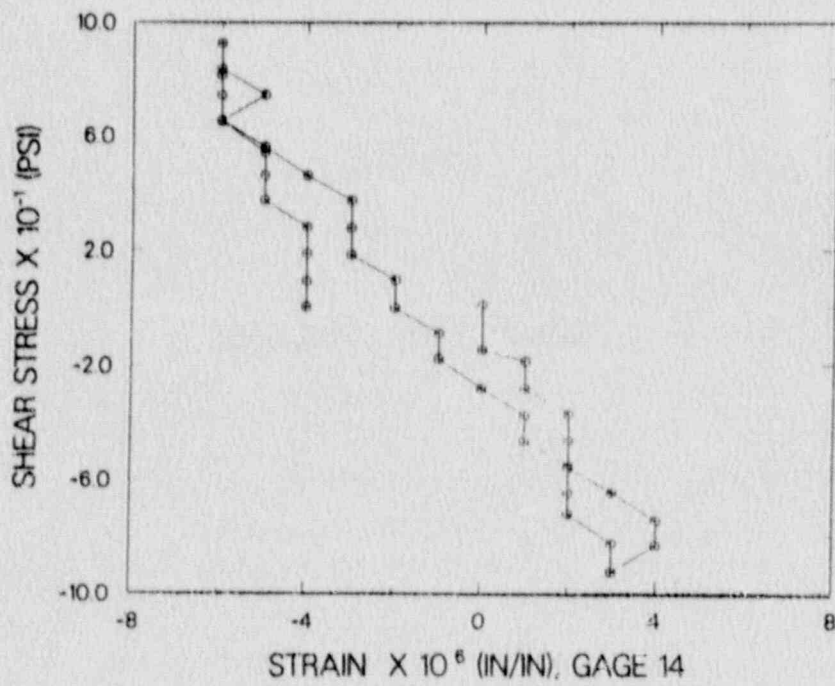
Fig. 26. Vertical strain in Gage 14, second 100-psi ABSS cycle.

29
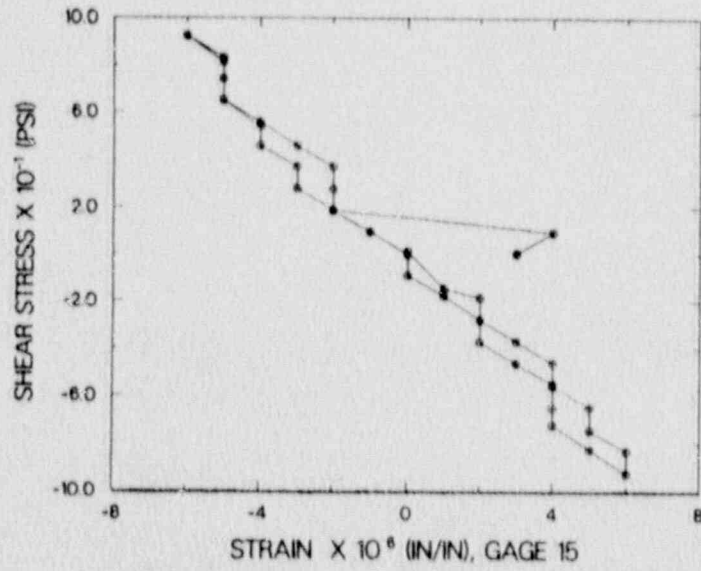
Fig. 27. Vertical strain in Gage 15,
second 100-psi ABSS cycle.
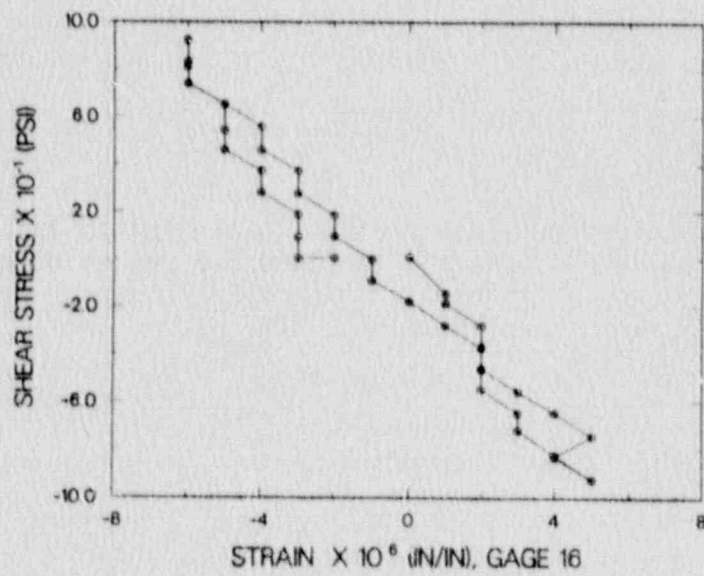
Fig. 28. Vertical strain in Gage 16,
second, 100-psi ABSS cycle.
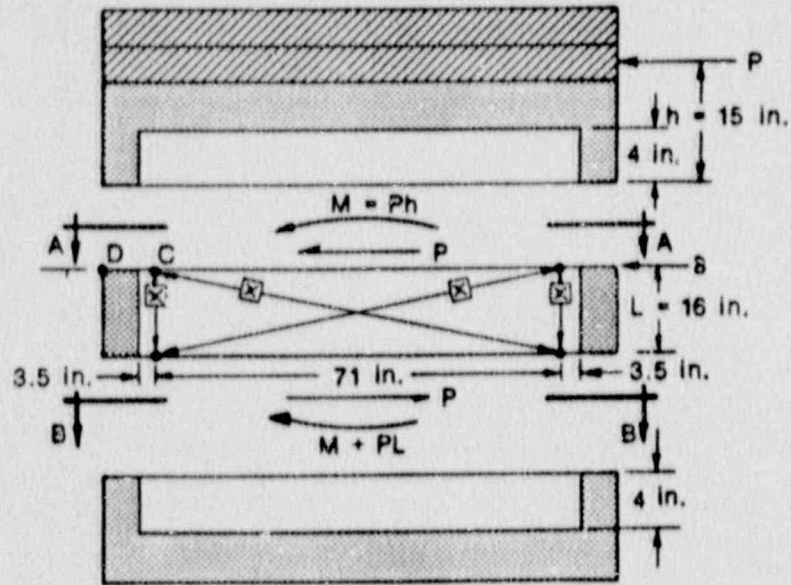
Fig. 29. Free-body diagram of TRG-6.

where

U	=	internal strain energy,
M	=	moment at section A-A,
P	=	shear force at section A-A,
δ	=	imaginary unit load,
E	=	concrete modulus of elasticity,
I	=	cross-sectional moment of inertia, includes entire end wall but neglects steel,
G	=	shear modulus,
A_e	=	effective shear area, and
L	=	length of the wall between planes A-A and B-B.

Using standard procedures described in Popov,[18] the horizontal displacement of the structure at plane A-A relative to plane B-B can be determined and the stiffness of this portion of the structure can be expressed as

$$K_T = \frac{1}{\frac{hL^2}{2EI} + \frac{L^3}{3EI} + \frac{L}{A_e G}}$$

31

This total stiffness may be decomposed into a bending component and a shear component yielding

$$K_B = \frac{6EI}{2L^3 + 3hL^2} \text{ , and}$$

$$K_S = \frac{A_e G}{L} \text{ .}$$

Table VI summarizes the various stiffness values that could be obtained for this test structure, depending upon how effective the end walls are assumed to be and also depending upon which value for modulus of elasticity is used. For this shear-dominated structure, the range is fairly narrow (from 48-55 x 10^6 psi).

TABLE VI
TRG-6 THEORETICAL STIFFNESS VALUES
(Neglecting Reinforcement)

Moment of Inertia \ Modulus of Elasticity	Ave. From Test Cylinder 3.45 x 10^6 psi	$57,000\sqrt{f'_c}$ 3.90 x 10^6 psi	$33w^{3/2}\sqrt{f'_c}$ 3.82 x 10^6 psi	Ultrasonic 3.2 x 10^6 psi
Full Section 2.78 x 10^6 in^4	K_T = 47.7 x 10^6	53.9 x 10^6	52.8 x 10^6	49.2 x 10^6
	K_B = 2.92 x 10^9	3.30 x 10^9	3.23 x 10^9	3.01 x 10^9
	K_S = 48.5 x 10^6	54.8 x 10^6	53.7 x 10^6	50.1 x 10^6
ACI T Beam 7.46 x 10^5 in^4	K_T = 45.7 x 10^6	51.6 x 10^6	50.6 x 10^6	47.1 x 10^6
	K_B = 7.83 x 10^8	8.86 x 10^8	8.67 x 10^8	8.08 x 10^8
	K_S = 48.5 x 10^6	54.8 x 10^6	53.7 x 10^6	50.1 x 10^6
Neglect Flange 3.645 x 10^5 in^4	K_T = 43.0 x 10^6	48.7 x 10^6	47.7 x 10^6	44.4 x 10^6
	K_B = 3.83 x 10^8	9.33 x 10^8	4.24 x 10^8	3.95 x 10^8
	K_S = 48.5 x 10^6	54.8 x 10^6	53.7 x 10^6	50.1 x 10^6

VIII. OTHER INVESTIGATORS' RESULTS

Figures 30-32 provide a summary of the available static test data for low-aspect-ratio reinforced concrete shear walls. These figures compare other investigators' results and the results obtained in the Seismic Category I Structures Program.

The measured secant stiffness vs. theoretical (SOM) stiffness is plotted in Fig. 30 before first cracking. Most test data on actual concrete test specimens, including the structure tested in this investigation, indicate that, prior to cracking, an SOM analysis gives an accurate prediction of the shear wall's stiffness. Microconcrete, however, seems to show a considerable
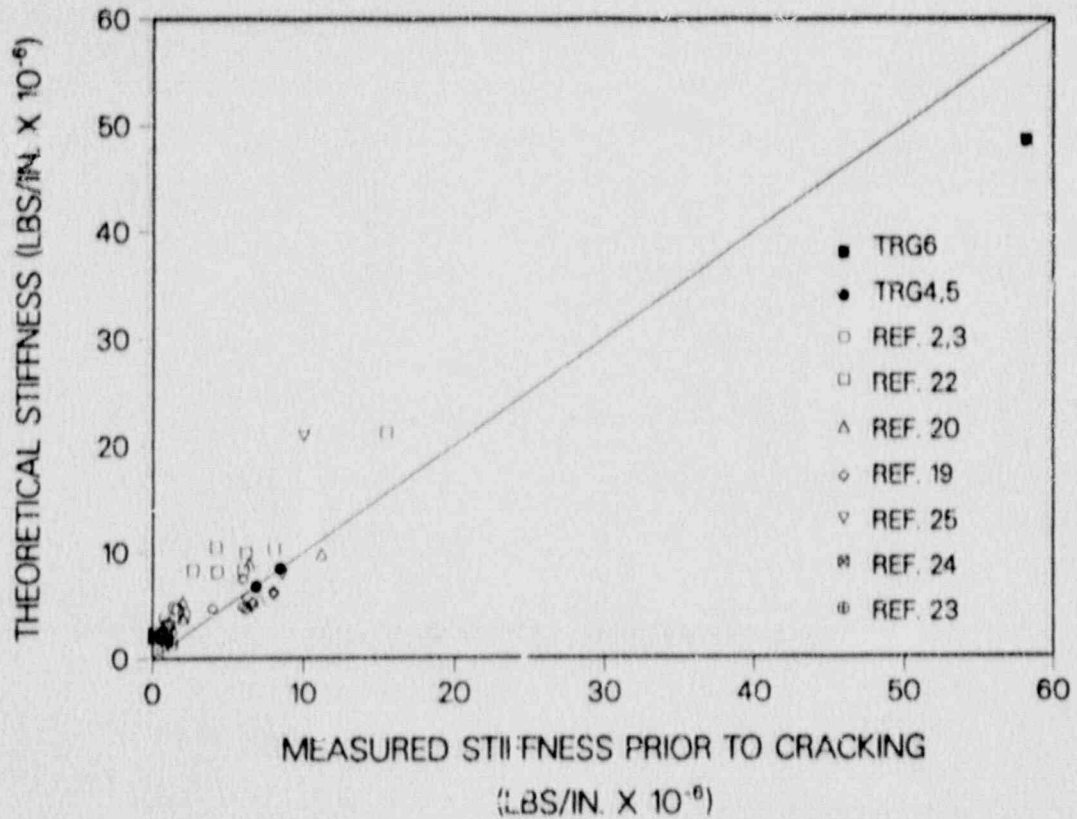
Fig. 30. Comparison of other investigators' results with TRG-6
results of measured stiffness versus theoretical stiffness.
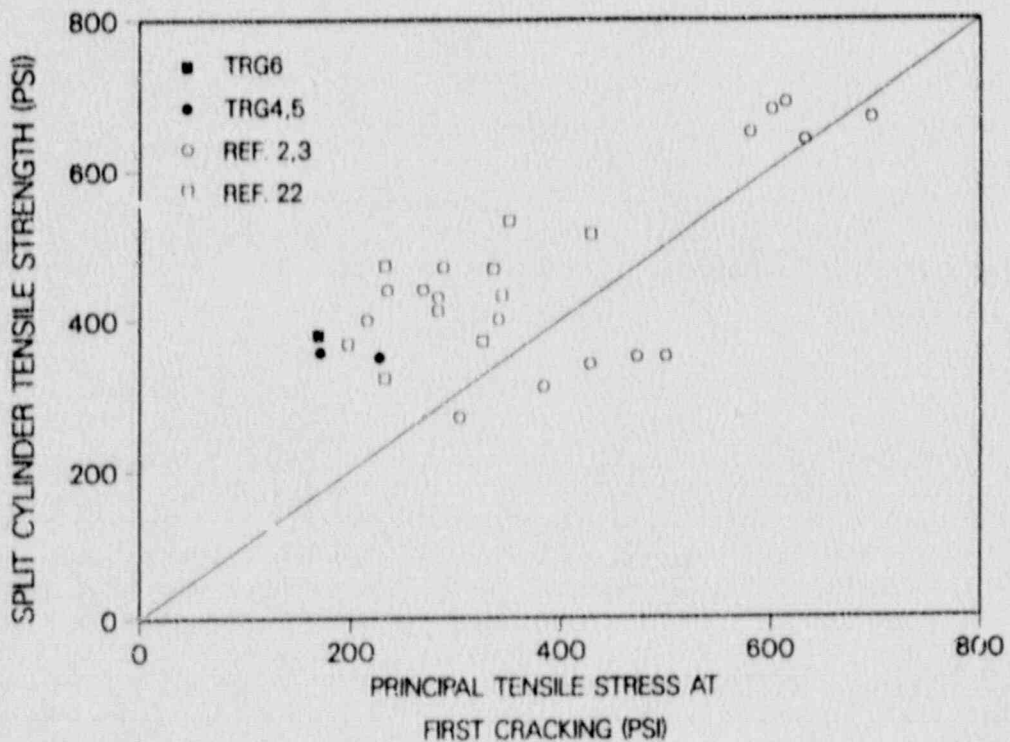

Fig. 31. Comparison of other investigators' results with TRG-6 results;
principal tensile stress at first cracking versus split cylinder
tensile strength.

reduction in stiffness prior to the first-cracking load. There are several investigations of actual concrete structures that show similar reductions in stiffness prior to cracking, as were observed in the Los Alamos microconcrete models.

Figures 31 and 32 compare the principal tensile strength at first-cracking with the split cylinder tensile strength and ACI 349's empirical tensile strength value of $4\sqrt{f_c'}$, respectively. These figures show that TRG-6 cracked at stress levels similar to the previous TRG structures. Data for Figs. 30-32 were obtained from Refs. 2,3,6,7, and 19-25.
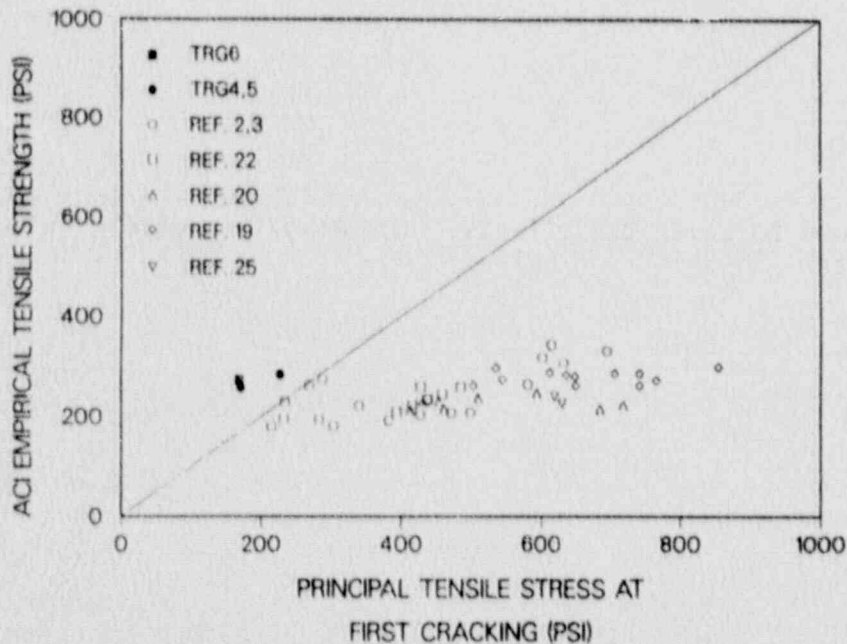
Fig. 32. Comparison of other investigators' results with TRG-6 results; principal tensile stress at first cracking versus ACI-349 principal tensile strength.

IX. CONCLUSIONS

One of the primary purposes of this test was to determine if, during a carefully monitored static load cycle test, a stiffness reduction of 4 would occur at similar load levels as have been observed in dynamic tests. During the pre-cracking load cycles and the low-level modal analysis, no stiffness reduction was observed, and the measurements indicated a stiffness slightly higher than theory would predict. The precracking response of the structure was accurately predicted with currently used linear analysis techniques based on strength of materials theory. These same techniques would not have adequately predicted the dynamic response of structures previously tested in the program, even though stress levels during the dynamic tests were well below those predicted to crack the structure.

34

Based upon the quasi-cyclic testing of TRG structures 4, 5 and 6, it is readily apparent that carefully handled structures tested fairly "green" (i.e., unaged), are uncracked, and can be accurately predicted by strength-of-materials theory.

The most likely cause of the reduced stiffness that has been measured in this program is concrete cracking. The source of this cracking has probably been (in our tests), a combination of several causes that include handling and transportation loadings in the early tests, aging (curing), shrinkage, and other time effects, and the construction imperfections and material variability that exist in all fabricated structures. However, we generally believe that the same cracking effects exist in real reinforced concrete structures because of many of the same reasons (handling and transportation loadings can be replaced by "differential settlement"). At least two courses of action should be pursued to further investigate this effect. First, if at all possible, data should be obtained from an actual nuclear plant structure. The instrumentation and testing should be designed to look particularly for this effect. Second, a "consequences" program should be initiated to see if any equipment will be affected by the frequency shifts and stiffness reductions measured in this program. Finally, the current method of treating these structures using an uncracked cross section for determining the structural element parameters and resulting floor response spectra should be re-examined and more realistic guidelines established to cover the effects. Los Alamos is working with professional society committees in this re-examination.

X. REFERENCES

1. E. G. Endebrock, R. C. Dove, and C. A. Anderson, "Margins to Failure - Category I Structures Program: Background and Experimental Program Plan," Los Alamos National Laboratory report, NUREG/CR-2347, December 1981.

2. E. G. Endebrock, R. C. Dove, and W. E. Dunwoody, "Analysis and Tests on Small-Scale Shear Walls, FY-82 Final Report," Los Alamos National Laboratory report, NUREG/CR-4274, September 1985.

3. R. C. Dove, J. G. Bennett, C. R. Farrar, and C. A. Anderson, "Seismic Category I Structures Program: Results for Fiscal Years 1983-84, FY 83-84 Report," Los Alamos National Laboratory report, NUREG/4924, September 1987.

4. R. C. Dove and J. G. Bennett, "Scale Modeling of Reinforced Concrete Category I Structures subjected to Seismic Loads," Los Alamos National Laboratory report, NUREG/CR-4474, (January, 1986).

5. R. C. Dove, E. G. Endebrock, W. E. Dunwoody, and J. G. Bennett, "Seismic Tests on Models of Reinforced Concrete Category I Buildings," Proc. Int. Conf. Structural Mechanics in Reactor Technology, 8th, Brussels, 1985.

6. J. G. Bennett, R. C. Dove, W. E. Dunwoody, C. R. Farrar, "Seismic Category I Structures Program: Results for FY 85," Los Alamos National Laboratory report, NUREG/CR-4998, December 1987.

7. J. G. Bennett, R. C. Dove, W. E. Dunwoody, C. R. Farrar, P. Goldman "Results for FY 1986 NUREG/CR-5182, September 1988.

8. ACI Committee 349, Code Requirements for Nuclear Safety Related Concrete Structures and Commentary, (American Concrete Institute, Detroit, 1985).

9. ACI Committee 318, Building Code Requirements for Reinforced Concrete (American Concrete Institute, Detroit, 1983).

10. "Standard Test Method for Slump of Portland Cement Concrete," in Annual Book of ASTM Standards, Roberta A. Prieman-Storer, Ed. (American Society for Testing and Materials, Philadelphia, PA, 1985), Vol. 4.02, C-143-78, pp. 109-112.

11. "Method of Sampling Freshly Mixed Concrete," in Annual Book of ASTM Standards, Roberta A. Prieman-Storer, Ed. (American Society for Testing and Materials, Philadelphia, PA 1985), Vol. 4.02, C-172-82, pp. 133-135.

12. "Standard Method of Making and Curing Concrete Specimen in the Field," in Annual Book of ASTM Standards, Roberta A. Prieman Storer, Ed. (American Society for Testing and Materials, Philadelphia, PA 1985), Vol. 4.02, C31-84, pp. 5-10.

13. "Specification for Concrete Aggregates," in Annual Book of ASTM Standards, Roberta A. Prieman-Storer, Ed. (American Society for Testing Materials, Philadelphia, PA 1985), Vol. 4.02, C33-85, pp. 11-20.

14. "Standard Test Method for Compressive Strength of Cylindrical Concrete Specimen," in Annual Book of ASTM Standards, Roberta A. Prieman-Storer, Ed. (American Society for Testing and Materials, Philadelphia, PA, 1985), Vol. 4.02, C-39-84, pp. 24-29.

15. "Standard Test Method for Static Modulus of Elasticity and Poisson's Ratio of Concrete in Compression," in Annual Book of ASTM Standards, Roberta A. Prieman-Storer, Ed. (American Society for Testing and Materials, Philadelphia, PA, 1985), Vol. 4.02, C469-83, pp. 303-307.

16. "Standard Test Method for Splitting Tensile Strength of Cylindrical Concrete Specimens," in Annual Book of Standards, Roberta A Prieman-Storer, Ed. (American Society for Testing and Materials, Philadelphia, PA, 1985), Vol. 4.02, C496-85, pp. 335-339.

17. T. R. Naik, "Ultrasonic Testing of Concrete," in Experimental Methods In Concrete Structures for Practitioners, G. M. Sabnis and N. Fitz Simmons, Eds. (American Concrete Institute, Detroit, 1979).

18. E. P. Popov, Introduction to Mechanics of Solids (Prentice-Hall, Englewood Cliffs, N.J., 1969).

19. G. D. Galletly, "An Experimental and Analytical Investigation of Reinforced Concrete Shear Panels," Ph.D. Thesis, Dept. of Civil and Sanitary Eng., Mass. Int. Tech., Cambridge, Mass., 1952.

20. J. R. Benjamin and H. A. Williams, "The Behavior of One-Story Reinforced Concrete Shear Walls," J. Structural Division, ASCE, 83, No. ST3, Proc. Paper 1254, pp. 1254-1 to 1254-49 (May 1957).

21. J. Antebi, "Model Analysis of the Response of Shear Walls to Dynamic Loads," Ph.D. Thesis, Dept. of Civil and Sanitary Eng., Mass. Inst. Tech., Cambridge, Mass., 1961.

22. F. Barda, "Shear Strength of Low-Rise Walls with Boundary Elements," Ph.D. Thesis, Dept. of Civil Eng., Lehigh Univ., Bethlehem, PA, 1972.

23. V. Cervenka and K. H. Gerstle, "Inelastic Analysis of Reinforced Concrete Panels: Experimental Verification and Application," Publ. Int. Ass. Bridge and Structural Eng., 32-II, 25-40 (1972).

24. A. E. Cardenas, H. G. Russell, and W. G. Corley, "Strength of Low-Rise Structural Walls," in Reinforced Concrete Structures Subjected to Wind and Earthquake Forces, J. Schwaighofer and S. Otani, Eds. (ACI SP-63, Detroit, 1980), pp. 221-241.

25. S. Wiradinata, "Behavior of Squat Walls Subjected to Load Reversals," Masters Thesis, Univ. of Toronto, Toronto, Canada, 1985.

APPENDIX A

ALBUQUERQUE TEST LABORATORY REPORT

TRG #6
Truck No. 1

Cylinder No. 7
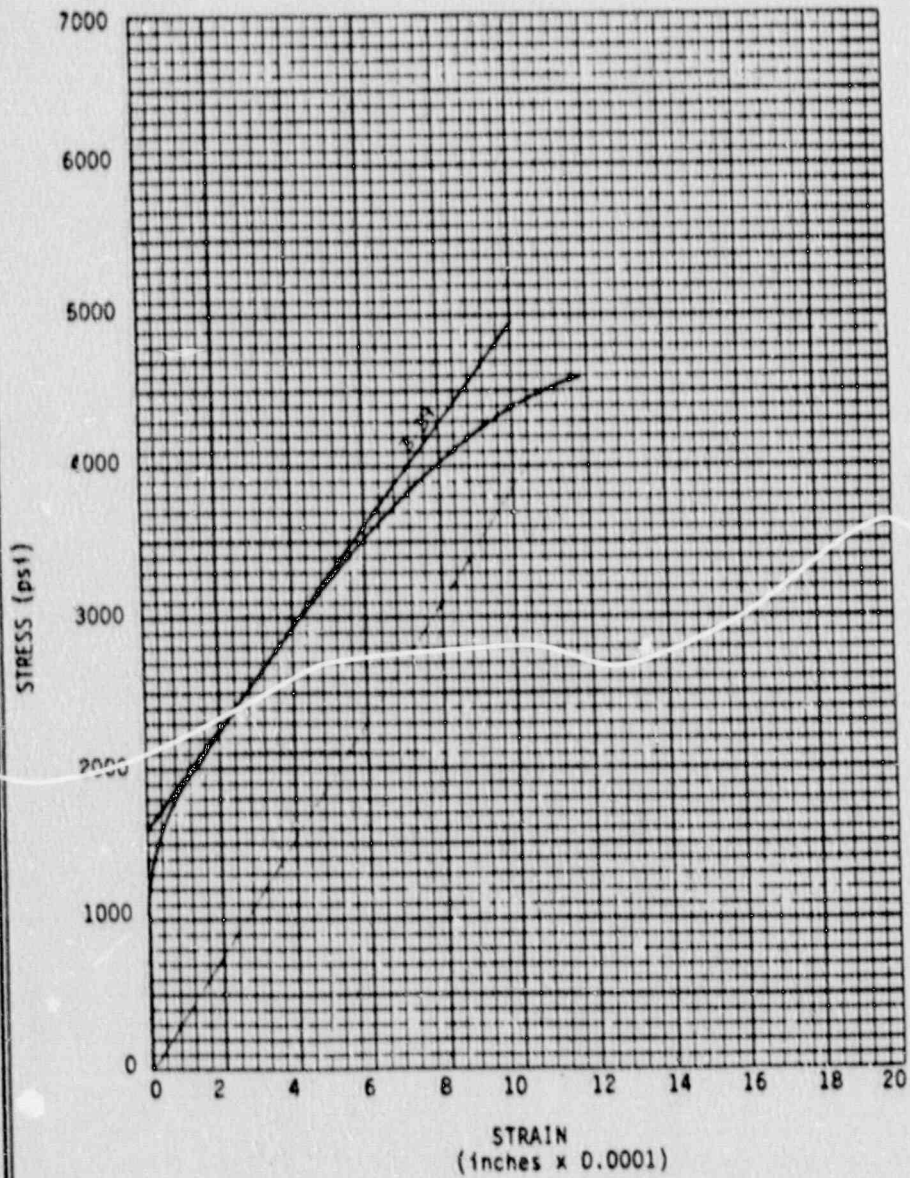
STRESS (psi)

7000

6000

5000

4000

3000

2000

1000

0

0 2 4 6 8 10 12 14 16 18 20

STRAIN
(inches x 0.0001)

PROJECT NAME	$E = 5.900 \times 10^6$	
Concrete Testing Los Alamos Labs Los Alamos, NM	Ult. Compressive Strength = 4740 psi	
	PROJECT NO	DATE
	531-70177-1	9/26/87

TRG #6
Truck No. 1
Cylinder No. 6

STRESS (psi)

STRAIN
(inches x 0.0001)
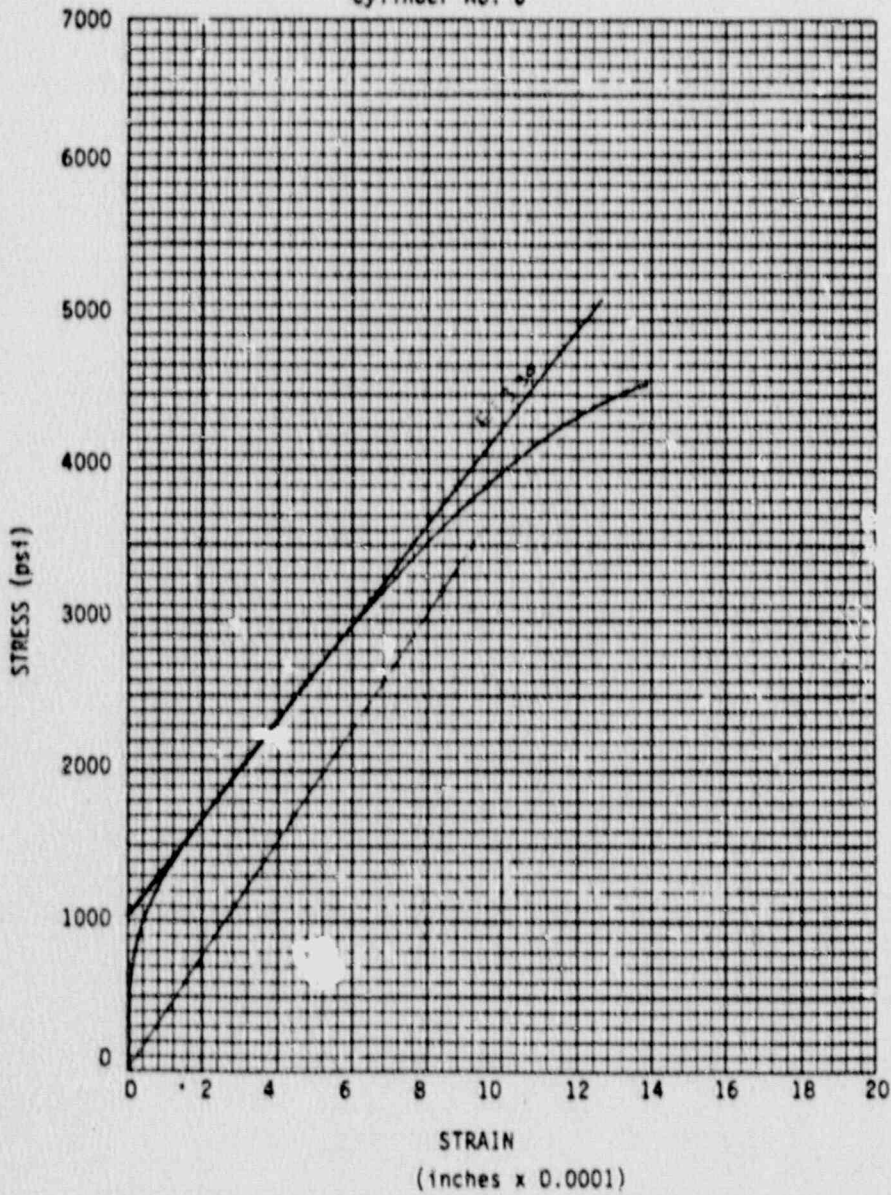
PROJECT NAME			
Concrete Testing Los Alamos Labs Los Alamos, NM	$E = 3.913 \times 10^6$ Ult Compressive Strength = 4880 psi		
	PROJECT NO 531-70177-1	DATE 9/26/87	

40

TRG #6
Truck No. 1
Cylinder #5
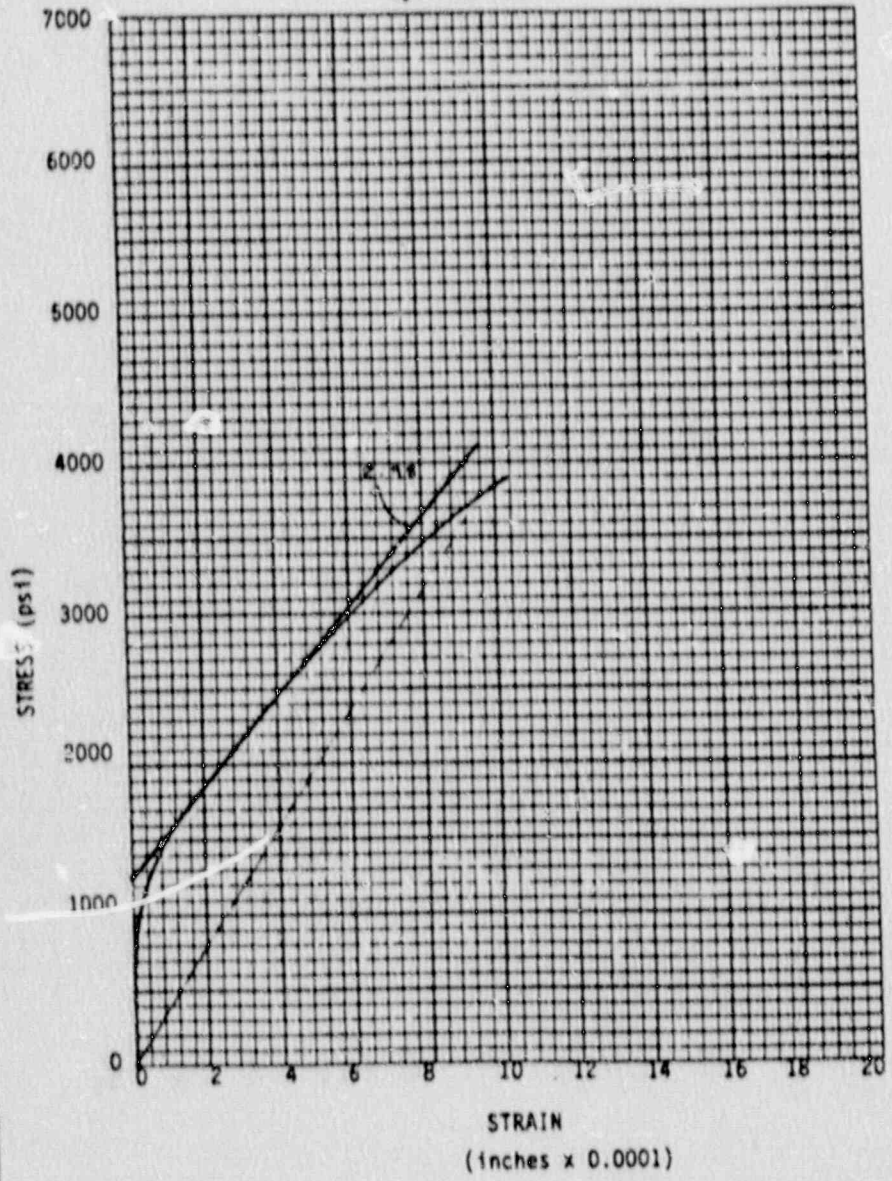
PROJECT NAME	$E = 4.778 \times 10^6$	
Concrete Testing Los Alamos Labs Los Alamos, NM	Ult. Compressive Strength = 4170 psi	
	PROJECT NO 531-70177-1	DATE 9/26/87

TRG #6
Truck No. 1
Cylinder No. 4

STRAIN
(inches x 0.0001)

PROJECT NAME	$E = 3.827 \times 10^6$	
Concrete Testing	Ult. Compressive Strength = 4865 psi	
Los Alamos Labs	PROJECT NO	DATE
Los Alamos, NM	531-70177-1	9/26/87

TRG #6

Truck No. 1
Cylinder No. 3

STRESS (psi) vs STRAIN (inches x 0.0001)

PROJECT NAME		
Concrete Testing Los Alamos Labs Los Alamos, NM	$E = 5.042 \times 10^6$	
	Ult. Compressive Strength = 4635 psi	
	PROJECT NO 531-70177-1	DATE 9/26/87

TRG #6
Truck No. 1
Cylinder No. 2

STRESS (psi)

STRAIN

(inches x 0.0001)

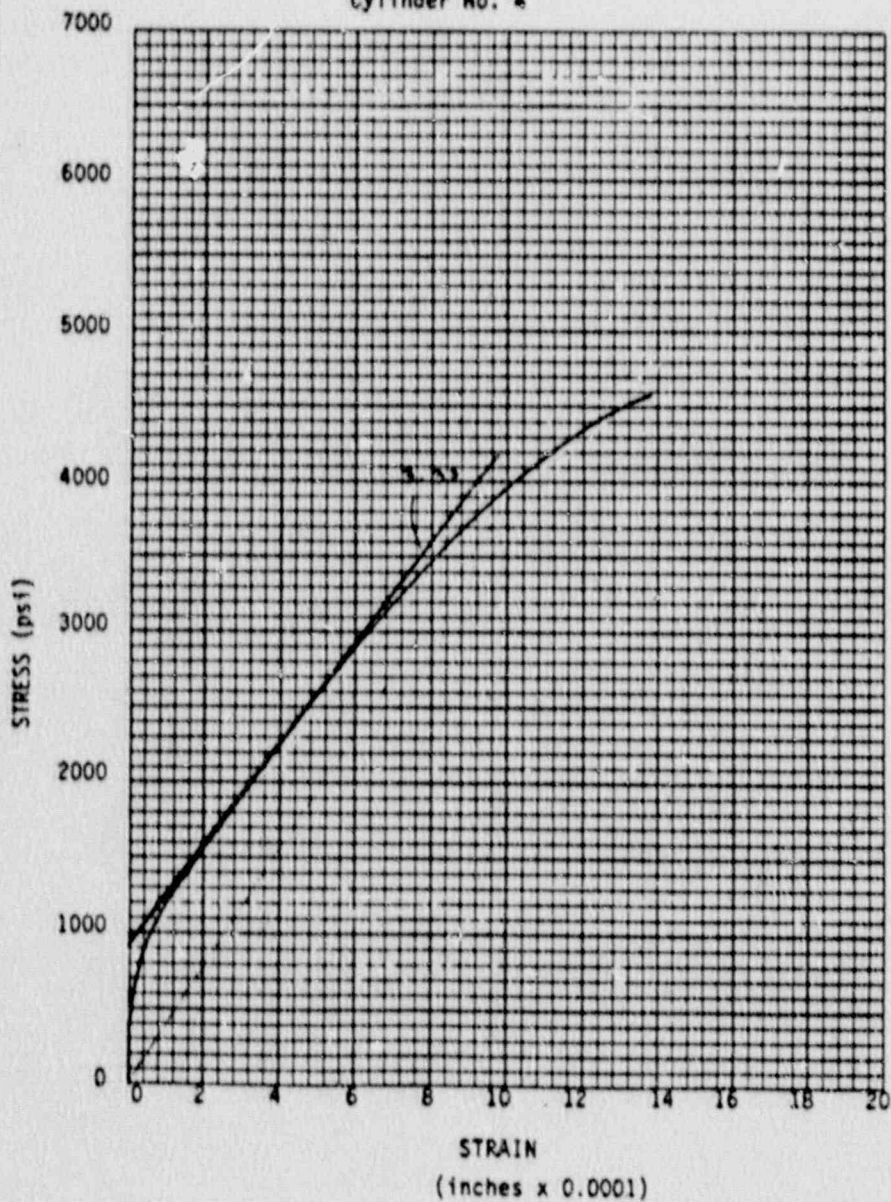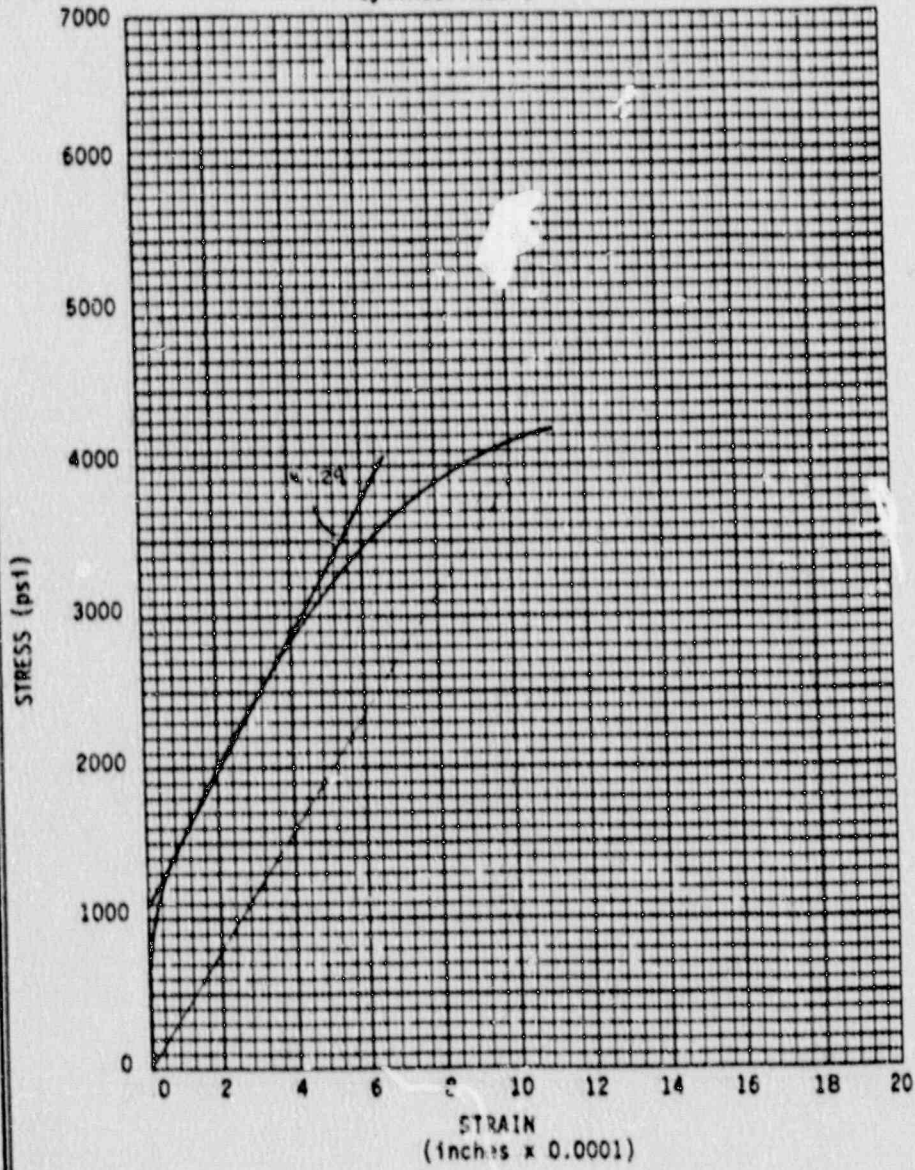| PROJECT NAME		
Concrete Testing Los Alamos Labs Los Alamos, NM	$E = 4.769 \times 10^6$ Ult. Compressive Strength = 4705 psi	
	PROJECT NO 531-70177-1	DATE 9/26/87

TRG #6
Truck No. 1
Cylinder No. 1
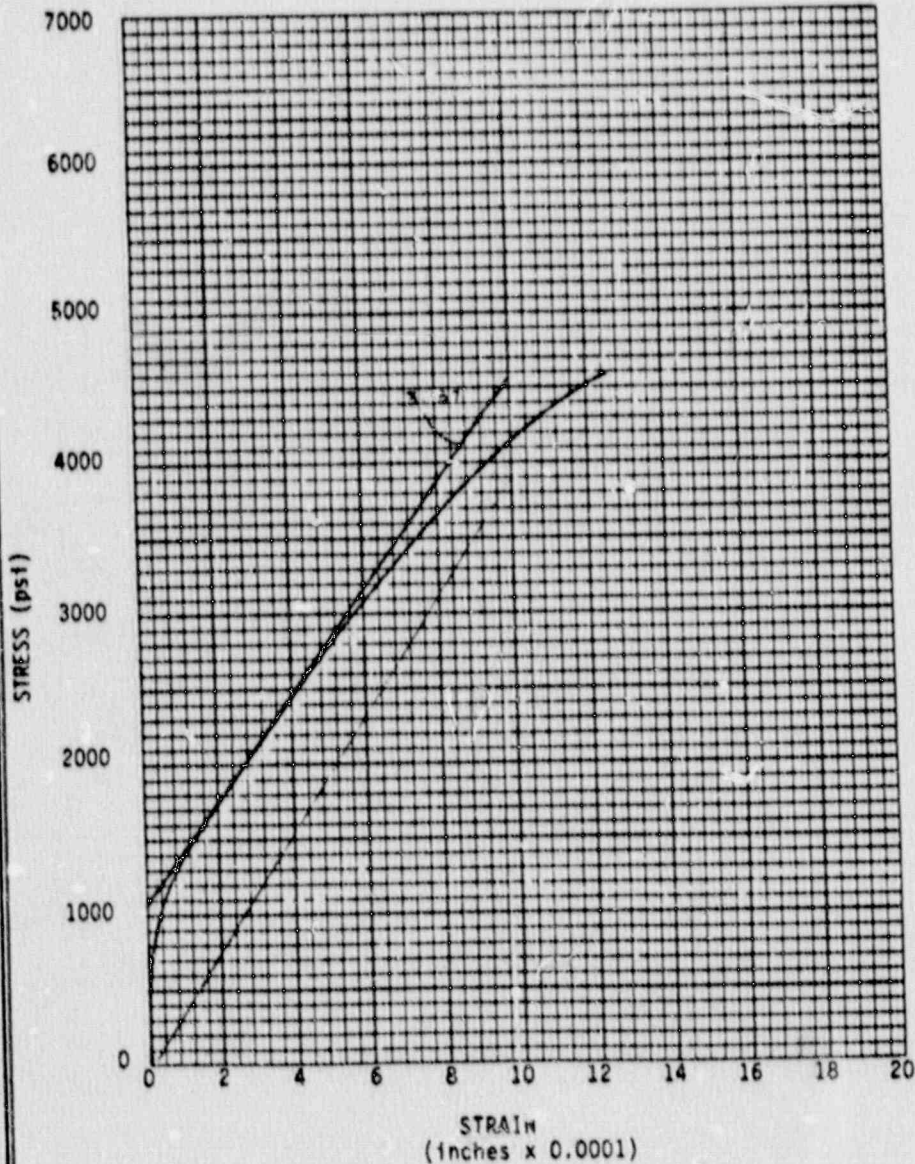
PROJECT NAME

Concrete Testing
Los Alamos Labs
Los Alamos, NM

$E = 4.048 \times 10^6$

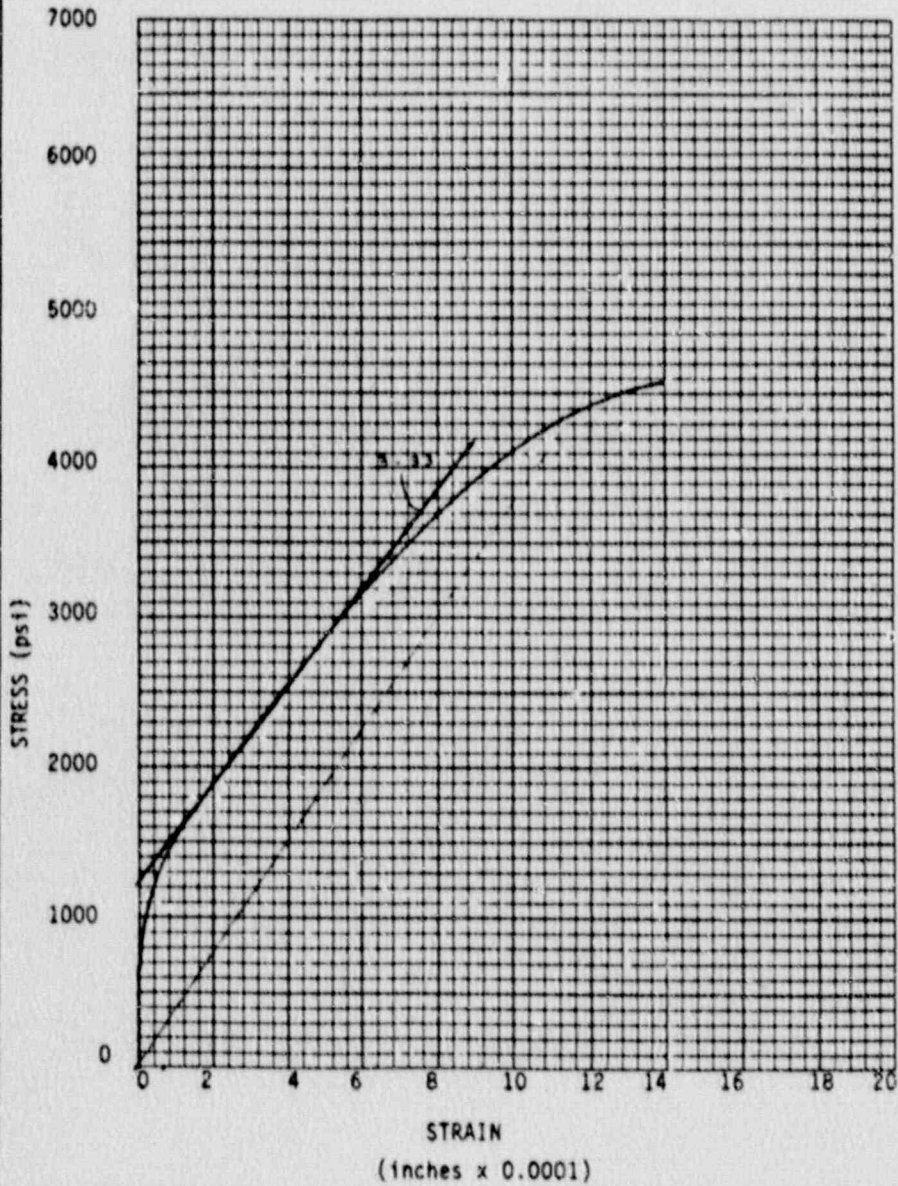Ult. Compressive Strength = 4860 psi

PROJECT NO	DATE
531-70177-1	9/26/87

Client: Los Alamos Labs
Project No. 531-70177
Project Name: Concrete Testing
Date: September 26, 1987

REPORT OF SPLIT TENSILE TESTS

TRG #6, Truck No 1

Cylinder Number	Unit Weight (pcf)	Split tensile Strength (psi)
1	141.3	355
2	141.6	420
3	140.6	380
4	142.3	360
Average:	141.5	380

APPENDIX B

LUKE SNELL TEST REPORT

◢LUKE M.◼◣
◢◼SNELL, P.E.◤

CONSTRUCTION & MATERIALS CONSULTANT

September 3, 1987

Joel Bennett
Los Alamos National Laboratory
MS J576
Los Alamos, NM 87545

Subject: Inspection of TRG-5 and TRG-6 Models
          Los Alamos National Laboratory
          Los Alamos, New Mexico
          Our Job No. LS87-354

Gentlemen:

The writer has completed the inspection of the above referenced models. The purpose of this inspection was to determine the uniformity of the concrete and to determine if the concrete contained flaws. This report documents our findings.

On August 24 and 25, 1987, the writer examined the TRG-5 and TRG-6 models. The examination consisted of two separate inspections. The first was a visual inspection using hand-held magnifying glasses. The second inspection was to determine the velocities of ultrasonic waves through the concrete.

The velocity of the ultrasonic wave was determined by measuring the wall thickness and measuring the time for the ultrasonic wave or a pulse to travel from a sending transducer, through the concrete to a receiving transducer; the velocity of the ultrasonic wave or the pulse velocity was then calculated by: pulse velocity = distance divided by time.

Past experience and research has shown that the pulse velocity value can be related to concrete strength and the static modulus of elasticity. Also, if the pulse velocities are relatively uniform, then the concrete is assumed to be of uniform quality and without flaws.

The equipment is generically called pulse velocity equipment. Our equipment is manufactured by James Electronic Company and is called the V-meter. The testing of each model will be discussed separately.

48

Model TRG-5

During our testing the following was determined:

1. The visual inspection indicated that the model had several internal and external voids that had been repaired. Several of these repairs appeared to be satisfactory. Other repairs were poorly bonded to the concrete and were easily remov⌐⌐. Several surface voids were also noted. The model does not appear to have internal voids that had not been repaired.

2. Test cylinders: Four concrete test cylinders were examined to determine their pulse velocity. The cylinders were made from the two trucks that provided concrete to make the model. The pulse velocities ranged from 14,300 to 14,700 ft./sec. with an average velocity of 14,500 ft./sec.

3. Shear wall: 36 pulse velocities were determined for the shear wall. These pulse velocity ranged from 11,400 to 14,400 feet per second with an average of 13,100 feet per second.

4. Base: 4 pulse velocities were determined on the base. The pulse velocities ranged from 12,800 to 13,600 feet per second with an average velocity of 13,300 feet per second.

5. Roof: 8 pulse velocities were determined on the roof. The pulse velocities ranged from 12,300 to 13,300 feet per second with an average velocity of 13,000 feet per second.

6. Northwest Wing Wall: 20 pulse velocities were determined on this wing wall. These pulse velocities ranged from 12,800 to 14,300 feet per second with an average velocity of 13,400 feet per second.

7. Northeast Wing Wall: 20 pulse velocities were determined on this wing wall. These pulse velocities ranged from 12,000 to 14,300 feet per second with an average velocity of 13,200 feet per second.

8. Southwest Wing Wall: 20 pulse velocities were determined on this wing wall. These pulse velocities ranged from 12,400 to 14,900 feet per second with an average velocity of 13,600 feet per second.

9. Southeast Wing Wall: 20 pulse velocities were determined on this wing wall. These pulse velocities ranged from 13,200 to 14,100 feet per second with an average velocity of 13,700 feet per second.

The pulse velocities of the four concrete cylinders were nearly identical. This indicates that the concrete strength and static modulus of elasticity for each load of concrete would be similar.

The pulse velocities in the model were not uniform and were below the pulse velocities of the tested concrete cylinders. This indicates that the concrete in the model is not uniform and the test cylinders may not accurately describe the concrete strength and the modulus of elasticity of the model.

The use of pulse velocities to estimate compressive strength and static modulus of elasticity is inexact and should be used only to indicate approximate values. Using the generalized data developed from past research, the compressive strength of the model would be variable but should exceed 3,000 psi. The static modulus of elasticity would also be variable but should exceed 3,000,000 psi.

Model TRG-6

During our testing the following was determined:

1. Visual Inspection: The visual inspection indicated that this model did not appear to have external voids.

2. Test Cylinders: Two 6 x 12 inch cylinders were examined to determine pulse velocities. These pulse velocities had an velocity of 14,100 feet per second. There was no variation in the pulse velocity between cylinders.

3. Shearwall: 8 pulse velocities were determined for the shear wall. These pulse velocities ranged from 13,500 to 14,300 feet per second with an average of 13,900 feet per second.

4. Base: No readings were determined for the base.

5. Roof: 18 pulse velocities were determined on the roof. The pulse velocities ranged from 12,900 to 13,700 feet per second with an average velocity of 13,100 feet per second.

6. Wing Walls: 8 pulse velocities were determined on the wing walls. These pulse velocities ranged from 13,000 to 14,000 feet per second with an average velocity of 13,600 feet per second.

The pulse velocities in the model were fairly uniform and similar to the pulse velocities of the tested cylinders. This indicates that the concrete in the structure is of uniform

quality and that the concrete strength and static modulus of elasticity of the model can be accurately determined from the concrete cylinders.

Since the pulse velocities were fairly uniform and the visual inspection did not indicate any external flaws, it is our opinion that the concrete model does not contain internal flaws.

The use of pulse velocities to estimate compressive strength and static modulus ofelasticity is inexact and should be used only to indicate approximate values. Using the generalized data developed from past research, the compressive strength would be in excess of 3,000 psi and static modulus of elasticity would be in excess of 3,000,000 psi.

Conclusions

I was instructed that Model TRG-5 will have additional repairs to the surface flaws. In my opinion, these repairs (if well bonded and of comparable concrete strength) will eliminate some of the non-uniformity of the concrete in the model.
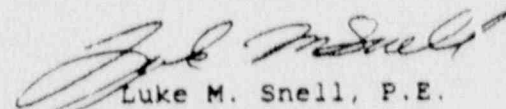
The variations of the pulse velocity in this model and the lower pulse velocities of the model to the test cylinders indicates that the concrete in the model is non-uniform and may be of lower strength than the test cylinders. The percent of repaired concrete is quite small (estimated to be less than 2%). If the repairs are successfully completed, its impact on the structural behavior would likely be insignificant.

The lower strength of the concrete in this model (as compared to the test cylinders) and the variation of the concrete may have an influence on the structural behavior.

Model TRG-6 appears to be well made and no apparent problems were noted. The concrete cylinders appear to be consistent with the concrete in the model and will be a good indication of the strength of the concrete in the model.

It has been a priviledge working with you on this project. If you have any questions or if we can be of future service, please do not hesitate to call.

Very truly yours,

Luke M. Snell, P.E.
Consultant

APPENDIX C

FIELD MEASUREMENTS FOR TRG-5

(This data was included because it was
part of Professor Snell's test report)

Cylinders (6 x 12 inch)

Truck #1	Time in 10^{-6} Seconds
Cylinder 1	68
Cylinder 2	70

Truck #2	
Cylinder 1	68
Cylinder 2	69

Shear Wall - Thickness = 4 inches

Readings on approximately 1' centers
Measured from base

Distance From Westwall (inches)	Time in 10^{-6} Seconds
10	23.2, 23.3, 24.1, 25.3, 27.9, 26.9
24	23.4, 23.5, 24.5, 25.9, 25.0, 24.9
36	24.1, 24.1, 24.3, 26.0, 25.7, 26.4
48	25.9, 27.1, 26.7, 26.9, 26.3, 26.4
60	25.5, 29.2*, 26.7, 26.9, 25.4, 25.3
72	25.1, 25.6, 25.1, 26.1, 25.3, 25.0

Test on Repair - 26.1

*Took several readings in this area. The shear wall in this area appears to have surface flaws.

Walls - Thickness = 4 inches

Readings on approximately one foot centers
Measured from Shear Wall

Distance from Base (in feet)	Time in 10^{-6} Seconds

Southwest Wall

1	24.4, 26.5, 25.1, 25.4
2	24.3, 25.7, 25.4, 23.5
3	23.3, 22.4, 24.1, 25.2
4	24.1, 23.0, 25.4, 24.8
6	24.4, 22.9, 23.1, 26.9

Northwest Wall

1	24.4, 24.9, 29.3, 24.4
2	25.1, 26.0, 24.9, 23.9
3	24.5, 25.8, 24.3, 25.3
4	25.4, 25.9, 24.4, 24.9
6	25.5, 23.3, 23.8, 24.9

Southeast Wall

1	23.7, 23.6, 23.7, 23.6
2	23.8, 24.4, 23.7, 23.6
3	23.7, 25.1, 23.3, 24.6
4	24.9, 25.0, 25.0, 24.3
6	23.8, 23.8, 23.3, 24.4

Northeast Wall

1	24.4, 24.5, 25.2, 24.9
2	24.9, 25.0, 25.1, 25.9
3	25.3, 24.8, 25.0, 24.9
4	26.8, 27.7, 25.5, 25.5
6	23.3, 23.8, 24.0, 24.7

Roof - Thickness = 8 inches

Location	Time x 10^{-6} Seconds
North	
At quarter points	54, 51, 50, 51
South	
At quarter points	51, 50, 50, 53

Base - Thickness = 8 inches

Location	Time x 10^{-6} Seconds
South	
At front quarter points	49, 52
North	
At front quarter points	51, 49

APPENDIX D

FIELD MEASUREMENTS FOR TRG-6

TRG-6

Roofs - Thickness = 8 inches

Readings on approximately 1.5 feet intervals
Measured from East Wall

North

Distance	Time x 10^{-6} Seconds
1 foot from opened end	49.5, 49.9, 49.6, 51.9
1 foot from shear wall	51.7, 50.4, 51.7, 51.6
2.5 feet from opening	50.1, -, -, 52.9

South

1 foot from open end	49.1, 48.5, 49.9, 51.9
1/2 foot from shear wall	52.5, 53.7, 51.5, 53.5

TRG-6 Shear Wall - Thickness = 8 inches

Readings on approximately 1.5 feet center
Measured from East Wall

Distance	Time x 10^{-6} Seconds
1 foot from roof	35.9, 35.7, 36.1, 37.1
1 foot from bottom	35.0, 36.1, 36.1, 35.9

TRG-6 Walls - Thickness = 6"

Readings on approximately 2 feet intervals
Measures from open end

Northwest

Distance	Time x 10^{-6} Seconds
1.5 feet from top	37.9, 38.4

Northeast

1.5 feet from top	36.7, 36.5

Southwest

1.5 feet from top	35.8, 36.8

Southeast

1.5 feet from top	36.5, 36.6

2. TITLE AND SUBTITLE

Static Load Cycle Testing of a Very Low-Aspect-Ratio Six-Inch Wall TRG-Type Structure TRG-6-6 (0.27, 0.50)

3. DATE REPORT PUBLISHED

MONTH	YEAR
November	1990

4. FIN OR GRANT NUMBER

A7221

5. AUTHOR(S)

C.R. Farrar, J.G. Bennett, W.E. Baker*, W.E. Dunwoody

6. TYPE OF REPORT

Technical

7. PERIOD COVERED (Inclusive Dates)

8. PERFORMING ORGANIZATION – NAME AND ADDRESS (If NRC, provide Division, Office or Region, U.S. Nuclear Regulatory Commission, and mailing address; if contractor, provide name and mailing address.)

Los Alamos National Laboratory
Los Alamos, New Mexico 87545

10. SUPPLEMENTARY NOTES *Consultant at Los Alamos. Mechanical Engineering Department, University of New Mexico, Albuquerque, NM 87131

11. ABSTRACT (200 words or less)

This test report is the third for a series of tests carried out by the Los Alamos National Laboratory under the sponsorship of the United States Nuclear Regulatory Commission's Division of Engineering. This research program has a Technical Review Group that recommended test geometries and sizes for the tests.

The quasi-static load cycle testing of a totally shear-dominated structure (bending deformation negligible) made of 6-inch-thick reinforced concrete walls is reported herein. The background of the program and the results that led to this series of experiments is first reviewed for continuity. Next, the geometry of the test structure, the design parameters, and the construction of the structure, including the material property tests, are reported. Both modal analysis and modal testing were done to verify the undamaged dynamic properties of the structure. Finally, the results of the quasi-static cyclic testing are reported in detail.

Results are compared with other investigations and with the American Concrete Institute (ACI) 349-85 code predictions.

12. KEY WORDS/DESCRIPTORS (List words or phrases that will assist researchers in locating the report.)

earthquake
building response
reinforced concrete structures
stiffness

13. AVAILABILITY STATEMENT

Unlimited

14. SECURITY CLASSIFICATION

(This Page)

Unclassified

(This Report)

Unclassified

15. NUMBER OF PAGES

16. PRICE

UNITED STATES
NUCLEAR REGULATORY COMMISSION
WASHINGTON, D.C. 20555

———

OFFICIAL BUSINESS
PENALTY FOR PRIVATE USE, $300

NUREG/CR-5553

STATIC LOAD CYCLE TESTING OF A VERY LOW-ASPECT-RATIO SIX-INCH WALL
TRG-TYPE STRUCTURE TRG-6-6 (0.27, 0.50)

NOVEMBER 1990